Microbiome

RESEARCH

Open Access

Anaerostipes caccae CML199 enhances bone development and counteracts aging-induced bone loss through the butyrate-driven gut–bone axis: the chicken model

Zhengtian Lyu[1], Gaoxiang Yuan[1], Yuying Zhang[1], Fengwenhui Zhang[1], Yan Liu[1,2], Yifan Li[1], Guang Li[1], Ying Wang[3], Ming Zhang[3], Yongfei Hu[1], Yuming Guo[1*] and Dan Liu[1*]

Abstract

Background The gut microbiota is a key regulator of bone metabolism. Investigating the relationship between the gut microbiota and bone remodeling has revealed new avenues for the treatment of bone-related disorders. Despite significant progress in understanding gut microbiota-bone interactions in mammals, research on avian species remains limited. Birds have unique bone anatomy and physiology to support egg-laying. However, whether and how the gut microbiota affects bone physiology in birds is still unknown. In this study, we utilized laying hens as a research model to analyze bone development patterns, elucidate the relationships between bone and the gut microbiota, and mine probiotics with osteomodulatory effects.

Results Aging led to a continuous increase in bone mineral density in the femur of laying hens. The continuous deposition of medullary bone in the bone marrow cavity of aged laying hens led to significant trabecular bone loss and weakened bone metabolism. The cecal microbial composition significantly shifted before and after sexual maturity, with some genera within the class Clostridia potentially linked to postnatal bone development in laying hens. Four bacterial strains associated with bone development, namely *Blautia coccoides* CML164, *Fournierella sp002159185* CML151, *Anaerostipes caccae* CML199 (ANA), and *Romboutsia lituseburensis* CML137, were identified and assessed in chicks with low bacterial loads and chicken primary osteoblasts. Among these, ANA demonstrated the most significant promotion of bone formation both *in vivo* and *in vitro*, primarily attributed to butyrate in its fermentation products. A long-term feeding experiment of up to 72 weeks confirmed that ANA enhanced bone development during sexual maturity by improving the immune microenvironment of the bone marrow in laying hens. Dietary supplementation of ANA for 50 weeks prevented excessive medullary bone deposition and mitigated aging-induced trabecular bone loss.

Conclusions These findings highlight the beneficial effects of ANA on bone physiology, offering new perspectives for microbial-based interventions for bone-related disorders in both poultry and possibly extending to human health.

Keywords Laying hens, Gut microbiota, Bone remodeling, *Anaerostipes caccae*, Butyrate

*Correspondence:
Yuming Guo
guoyum@cau.edu.cn
Dan Liu
liud@cau.edu.cn
Full list of author information is available at the end of the article

Graphical Abstract

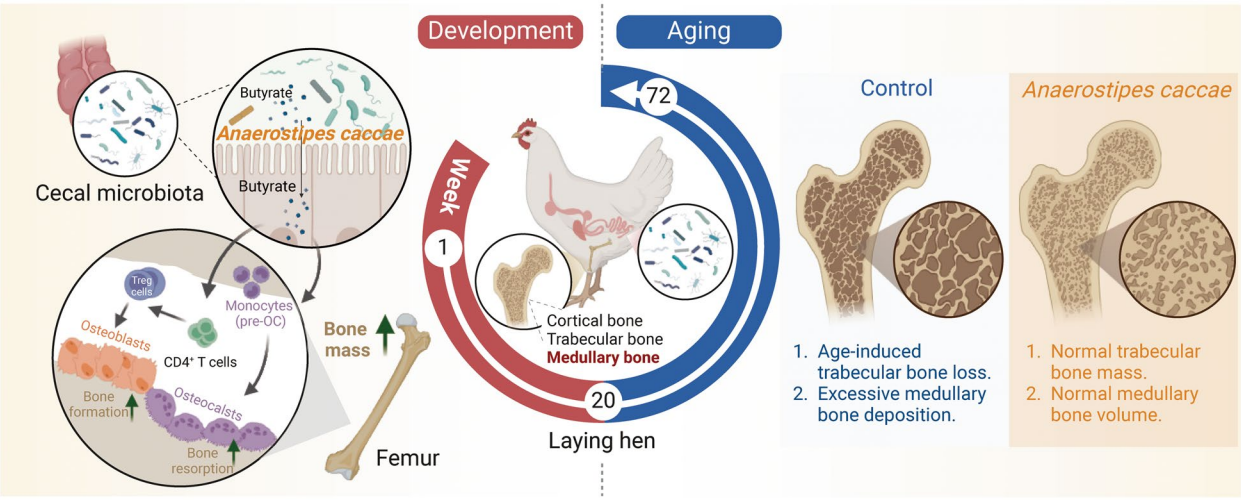

Background

In higher vertebrates, including birds and mammals, bones serve as mineralized, multifunctional organs within the skeletal system [1]. They are crucial for supporting posture and locomotion, protecting internal organs, maintaining mineral metabolic balance, and modulating endocrine functions [1–4]. Bone remodeling, a continuous process of renewal involving the removal of aged or damaged bone by osteoclasts and its replacement by new bone synthesized by osteoblasts, is essential for maintaining bone integrity [5, 6]. Achieving a balance between bone formation and resorption is crucial for avoiding net alterations in bone mass following remodeling [3, 6]. Disruption of this equilibrium can lead to a decline in bone functionality and conditions such as osteoporosis—a systemic skeletal disorder characterized by reduced bone mass and an increased risk of fractures [7–9]. Bone mass in later life is influenced by the maximum peak bone mass attained before adulthood and the rate at which bone is subsequently lost [10]. Bone loss occurs due to estrogen deficiency following menopause or through estrogen-independent pathways, including secondary hyperparathyroidism, chronic inflammation, and aging [5]. Thus, interventions aimed at enhancing peak bone mass and reducing bone loss are essential for the effective management of osteoporosis.

Medications for osteoporosis treatment are predominantly categorized into antiresorptive agents and anabolic agents [10]. However, the long-term use of certain medications is discouraged due to severe side effects, highlighting the need for safer treatments [11–13]. Recent studies on the role of gut microbiota in bone remodeling have revealed new prospects for osteoporosis treatment. Both artificial modifications to the microbiota and the impact of single-strain colonization underscore the complex relationship between gut microbiota and bone metabolism [14–22]. The gut microbiota influences bone metabolism both directly, by modulating bone remodeling through extracellular vesicles or secondary metabolites [23–26], and indirectly, by affecting bone remodeling via interactions with the immune and endocrine systems [27–30]. The need to discover novel probiotics with osteomodulatory effects is evident.

Despite significant advancements in comprehending the gut microbiota-bone remodeling nexus in rodents and humans, a conspicuous gap persists in avian species research. From a macrostructural standpoint, mammalian bones are classified into two categories: cortical bone and trabecular bone [31]. Distinctly, female birds have a specialized bone microarchitecture known as medullary bone, which is situated within the marrow cavities of long bones [32, 33]. This unique, nonstructured tissue acts as a dynamic calcium reservoir, known for its rapid and high-flux calcium metabolism [34, 35]. As economically vital poultry, laying hens exhibit highly active bone remodeling due to their daily egg-laying cycle, maintaining an egg production rate exceeding 90% from 22 to 45 weeks, with 10% of their total body calcium dedicated to eggshell formation daily, of which 20–40% is derived from medullary bone [35–37]. Notable fluctuations in the microarchitecture

of both medullary bone and trabecular bone throughout the oviposition cycle have been documented [35]. However, the specific developmental patterns of bones, especially medullary bone in hens, are still not well understood [38]. The debate continues on whether the prolonged and significant demand for calcium precipitates osteoporosis in hens. Additionally, poultry has a different gut microbiome compared with mammals to adapt to the shorter gastrointestinal tract [39]. Therefore, it is imperative to explore deeply the developmental patterns of laying hen bones and their link to the gut microbiota for novel scientific insights at the confluence of skeletal physiology and microbiology.

This study explores the developmental patterns of bone and the dynamic shifts in gut microbiota in laying hens as they age, further investigating the interplay between these two factors. We have identified four bacterial strains linked to bone development and evaluated their osteomodulatory effects on pseudo-sterile chicks and primary chicken osteoblasts. Among these, *Anaerostipes caccae* CML199 (ANA) exhibits the most substantial promotion of bone formation both *in vivo* and *in vitro*, attributed chiefly to its metabolite, butyrate. The inclusion of vacuum freeze-dried ANA powder in the diet not only fosters postnatal bone development but also counteracts aging-induced bone loss in laying hens. An overview of the experimental design is presented in Fig. 1.

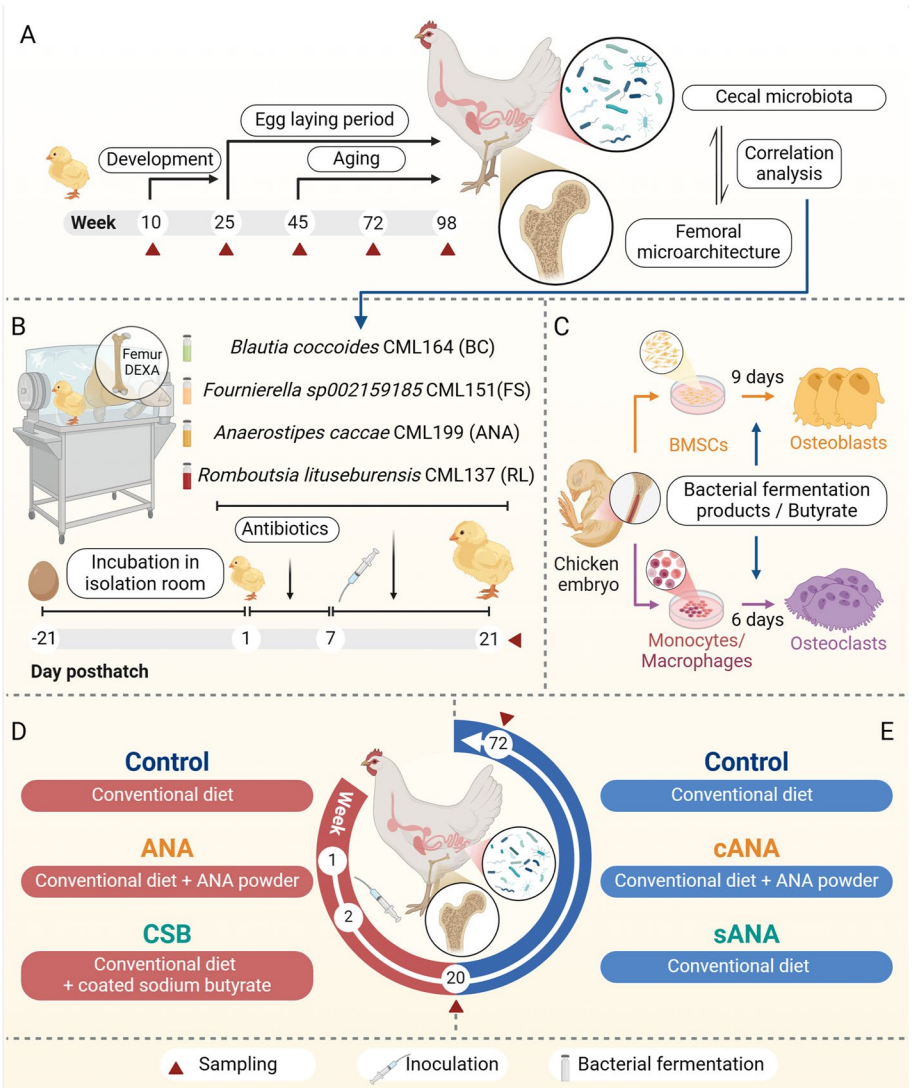

Fig. 1 Overview of the experimental design. Created with BioRender.com

Methods

Animals

For the experiments depicted in Fig. 1A, the LOHMANN PINK layers were sourced from Sichuan Sundaily Farm Ecological Food Co., Ltd. (Mianyang, China). Fifteen healthy laying hens at various stages of their laying cycle (10, 25, 45, 72, and 98 weeks) were humanely euthanized. Tissue samples (bones and cecal contents) were immediately frozen in liquid nitrogen and stored at − 80°C for subsequent analysis. For the experiments shown in Fig. 1B, Arbor Acres breeding eggs were obtained from Beijing Dafa Chia Tai Co., Ltd. (Beijing, China) and housed in a breeding base in Zhuozhou, Hebei Province, China. The feed was formulated according to the instructions of the Chinese chicken feeding standard (NY/T-33–2004). The feed composition and nutrient levels are presented in Table S2. As shown in Fig. 1C, 18-day-old breeding eggs were procured from Zhuozhou Mufeng Poultry Co., Ltd. (Zhuozhou, China). As shown in Fig. 1D, E, Jingfen No. 6 commercial pullets were purchased and maintained at the Zhuozhou breeding facility of China Agricultural University (Zhuozhou, China). The feed composition and nutrient specifications are outlined in Table S3.

All birds in this study had ad libitum access to feed and water. The environmental conditions, including room temperature and humidity, were automatically regulated following standard feeding management practices.

Bacterial cultivation, isolation, and identification

The methodology for bacterial cultivation and isolation was adapted from our previous study [40]. The identity of each strain was confirmed by amplifying the 16S rRNA gene using primers 27F (5′-AGA GTT TGA TCA TGG CTC A-3′) and 1492R (5′-TAC GGT TAC CTT GTT ACG ACT T-3′). The genome of *Anaerostipes caccae* CML199 (ANA) was sequenced, and its genome map was constructed using Proksee (https://proksee.ca/. Accessed 1 September 2022).

Primary chicken bone marrow mesenchymal stem cell culture

This procedure is based on our previously described method [41]. Briefly, femurs and tibias were isolated from chicken embryos, and the attached muscles were removed. Following the removal of epiphyses, the medullary cavity was flushed using a 1-mL syringe. The cells were cultured in a basal medium composed of low-glucose Dulbecco's modified Eagle's medium (DMEM; 31,600, Solarbio, Beijing, China), 10% fetal bovine serum (FBS, v/v, NEWZERUM, Christchurch, New Zealand), and 1% penicillin/streptomycin (v/v, P1400, Solarbio, Beijing, China). Cells in culture medium were transferred to T75 flasks and incubated at 37°C with 5% CO_2 for 3 days to allow adherence.

Osteogenic differentiation of BMSCs and treatment

After 3 days of cultivation, the supernatant was discarded, and bone marrow mesenchymal stem cells (BMSCs) were passaged and reseeded at approximately 6×10^5 cells/mL in a new T75 culture flask for further passaging. For osteogenic differentiation, passage 3 BMSCs were seeded at approximately 10^5 cells/mL in 6-well plates (or 12-well plates). The culture medium used for mineralization included 50 μg/mL L-ascorbic acid (A8100, Solarbio, Beijing, China), 10 mM β-glycerophosphate disodium salt (G418953, Aladdin, China), and 0.01 μM dexamethasone (D8040, Solarbio, Beijing, China). To investigate the effect of bacterial metabolites on osteoblast mineralization, the differentiation medium was replaced with 0.001%, 0.01%, or 0.1% bacterial fermentation products in Gifu anaerobic medium (GAM, HB8518, Hope bio, China) or blank GAM. Mineralization was assessed through alizarin red S (ARS) staining after 9 days. To investigate the effects of ANA and sodium butyrate (NaB) on osteoblast differentiation and mineralization, the differentiation medium was replaced with 0.01%, 0.1%, or 1% ANA metabolites or 10^{-6} M, 10^{-5} M, or 10^{-4} M NaB (IS0190, Solarbio, Beijing, China). After 3 days, the cells were harvested for RNA extraction and alkaline phosphatase (ALP) activity measurement. After 9 days, the cells were subjected to mineralization assays.

Osteoclast differentiation of monocytes and treatment

For osteoclast generation, the supernatant was collected after 24 h of BMSC incubation. Following red blood cell lysis, the residual cells were reseeded at 2×10^5 cells/mL in high-glucose DMEM supplemented with 10% FBS, 1% penicillin/streptomycin, and 50 ng/mL macrophage colony-stimulating factor (M-CSF) (CB34, Novoprotein, Suzhou, China). After 48 h, differentiation into osteoclasts was initiated by introducing 100 ng/mL receptor activator of nuclear factor kappa-B ligand (RANKL) (CR06, Novoprotein, Suzhou, China) to the culture, along with 0.01%, 0.1%, and 1% ANA metabolites or 10^{-6} M, 10^{-5} M, and 10^{-4} M NaB. After 6 days, the cells were collected for the measurement of tartrate-resistant acid phosphatase (TRAP) activity.

Inoculation of bacterial strains

Post-disinfection with povidone-iodine, the breeding eggs were transferred to an incubator situated in a HEPA-filtered isolation room. The incubator and room underwent daily disinfection throughout the incubation period [40]. Chicks, matched by body weight and

numbering fifteen per batch, were relocated to sterile isolators for rearing after 21 days of hatching. For the initial 6 days, the chicks were provided with sterilized drinking water containing a combination of antibiotics (200 ppm ampicillin, 200 ppm metronidazole, 200 ppm neomycin, and 100 ppm vancomycin). Antibiotic treatment was discontinued on day 7, and from day 8 onwards, chicks were inoculated with sterile saline and bacterial strains *Blautia coccoides* CML164, *Fournierella sp002159185* CML151, ANA, and *Romboutsia lituseburensis* CML137 (1 mL/bird/day), each containing 10^7–10^8 CFU/mL. All feed was sterilized using cobalt irradiation. The weights of the chicks in each group were documented, and tissue samples were collected following 14 days of bacterial inoculation. The femur length on one side was measured using calipers, while the femur on the opposite side and the cecal contents were immediately frozen in liquid nitrogen and stored at − 80°C for further analysis. A concise experimental design is depicted in Fig. 1B.

Fermentation and vacuum lyophilization of ANA

The fermentation and powder preparation of ANA were conducted according to the protocol described in our previous studies [42, 43]. ANA was cultured in GAM broth at 37°C under anaerobic conditions (10% H_2, 10% CO_2, 80% N_2; Don Whitley Scientific DG250, West Yorkshire, United Kingdom) for 24 h. After incubation, the culture underwent centrifugation at 3,000×*g* for 30 min at 4°C, followed by washing the pellets with distilled water and the addition of 10% skimmed milk powder as a cryoprotectant. The mixture was then freeze-dried for 48 h to produce the powder. Finally, the concentration of ANA powder was assessed through serial dilution and plating on GAM agar. The viability of the freeze-dried bacteria approached nearly 1×10^{12} CFU/g, and the bacteria were preserved at − 80 °C until use.

Dietary supplementation of ANA powder and coated sodium butyrate in a cohort of growing and developing laying hens

A cohort of 450 1-day-old Jingfen No. 6 commercial pullets was categorized into three groups based on body weight, with each group comprising 10 replicates of 15 birds each. The birds in the control groups were administered normal saline. The dietary regimen for 20 weeks included a conventional diet for the control group, a conventional diet supplemented with 10^9 CFU of ANA powder per kg of feed (ANA group), or a conventional diet supplemented with 1.5 g of coated sodium butyrate (CSB, Adisseo Co., Ltd., Shanghai, China) per kg of feed (CSB group). During the initial 2 weeks, birds in the ANA group received live ANA inoculation (1 mL/bird/day) at a concentration of 10^7–10^8 CFU/mL every other day. At 20 weeks, hens with similar body weights and shank lengths from each group were selected for tissue collection. Blood samples were obtained from the brachial wing vein, allowed to clot at room temperature for 8 h without anticoagulant, and then centrifuged at 3000 rpm for 15 min. The serum was harvested and stored at − 20°C for subsequent assays. The femur and cecal contents were immediately frozen in liquid nitrogen and stored at − 80°C for further analysis. A concise experimental design is illustrated in Fig. 1D.

Effects of ANA on bone physiology in a cohort of laying hens after sexual maturity

Between 20 and 72 weeks, the cohort previously administered ANA was bifurcated into two groups: one continued with ANA powder supplementation in the conventional diet (cANA), and the other transitioned to a conventional diet without ANA supplementation (sANA). Each group comprised 5 replicates with 12 hens per replicate. Concurrently, 60 chickens from the control group were randomly allocated into 5 replicates, each containing 12 hens, with no change in their diet. Sample collection proceeded as previously described. A concise experimental design is depicted in Fig. 1E.

Dual-energy X-ray absorptiometry analysis

The bone parameters shown in Fig. 1B were assessed using InAlyzer by dual-energy X-ray absorptiometry (DEXA, MEDIKORS, Korea). BMD, BMC, and BV were measured in the right femur. Each scan contained the same biological replicate sample of different processing groups.

Micro-CT analysis

The right femurs of laying hens were scanned using micro-CT (NEMO, PINGSENG Healthcare Inc., Kunshan, China). To ensure consistency in the volume of interest (VOI) for subsequent analysis, the outermost side of the femur was used as a reproducible landmark, as shown in Figure S1A. For the femoral microarchitecture region, we analyzed 60 slices (3 mm) beginning with 60 slices below the landmark. Three-dimensional images were reconstructed for visualization using the provided software with a 1024×1024 matrix. Image segmentation employed an adaptive-iterative threshold approach to differentiate between medullary, cortical, and trabecular bone.

Determination of ALP activity

For the ALP activity assays, cells were rinsed with PBS and then scraped in 200 μL cell lysis buffer (P0013J, Beyotime, Shanghai, China). After a brief vortex lysis, the samples were centrifuged at 12,000 rpm for 15 min at

4 °C. A total of 100 μL of the supernatant was collected for the determination of ALP activity, and the rest of the supernatant was used for the determination of the total protein concentration. According to the manufacturer's instructions (P0321S, Beyotime, Shanghai, China), 50 μL of the reactive solution (para-nitrophenyl phosphate, pNPP) was added to 50 μL of sample and incubated at 37 °C for 30 min. The reaction was stopped with 100 μL of stop solution. The absorbance of the sample was measured at 405 nm, and the concentration of the remaining protein was measured using the BCA protein assay kit (P0009, Beyotime, Shanghai, China). The ALP activity was normalized to total protein, which was expressed as μM *p*-nitrophenol/g protein/min.

Determination of TRAP activity

Cell lysis and supernatant collection were performed as described above. According to the manufacturer's instructions (P0321S, Beyotime, Shanghai, China), 40 μL of pNPP plus 5 μL of tartaric acid solution was added to 40 μL of the sample and incubated at 37 °C for 30 min. The reaction was stopped with 160 μL of stop solution. The absorbance of the sample was measured at 405 nm. The TRAP activity was normalized to total protein, which was expressed as μM *p*-nitrophenol/g protein/min.

Measurement of mineralizationviaARS staining

For ARS staining, the cells were fixed with 95% ethanol for 30 min after being washed with PBS. Following further rinsing with PBS, the cells were stained with 1% (w/v) ARS (pH 4.2, IA5140, Solarbio, China) for 1 h at room temperature. Unincorporated dye was removed by washing with PBS, after which the plate was left to dry for imaging. Finally, the content of each well was solubilized with 2–5 mL of 10% (w/v) cetylpyridinium chloride (C129534, Aladdin, Shanghai, China) for 15 min. The absorbance was read at 560 nm.

ELISA

Serum estradiol was measured with a Chicken Estradiol ELISA Kit (ANG-E32143C, Angel Gene, Nanjing, China). Serum osteocalcin was measured with a Chicken OCN ELISA Kit (ANG-E32164C, Angel Gene, Nanjing, China). The serum C-terminal telopeptide of type I collagen was measured with a Chicken CTX-I ELISA Kit (ANG-E32233C, Angel Gene, Nanjing, China). All procedures were performed according to the manufacturer's instructions.

16S rRNA gene sequencing and analysis

The cecal contents of the chickens were collected for microbiome analysis. 16S rRNA gene sequencing was conducted by Biomarker Technologies Co., Ltd. (Beijing, China). The Shannon and Simpson indices were used to measure community diversity. Beta diversity was evaluated by principal coordinate analysis to classify multiple samples and further demonstrate the differences in species diversity between samples. Relative abundances at the genus level were statistically compared between the groups. Linear discriminant analysis (LDA) effect size (LEfSe) was used to identify the differences in microbial composition and to search for biomarkers with statistical differences between different groups. All analyses were performed using BMKCloud (https://international.biocloud.net/zh/dashboard. Accessed 26 September 2023). The co-occurrence networks were constructed using Spearman correlations to unravel specific correlations between bone parameters and genus-level bacterial taxa in all the samples.

Short-chain fatty acid analysis

Targeted metabolomics was performed to quantify the concentrations of short-chain fatty acids (SCFAs) in the cecal contents and bacterial fermentation products. After the cecal contents were thawed, a thorough vortex and mixing were performed. The samples were extracted with double-distilled water (4×volume). After centrifugation at 12,000×*g* for 15 min at 4°C, the supernatant was mixed with 25% (w/v) metaphosphoric acid solution at a ratio of 5:1 (v/v). The mixture was centrifuged at 12,000×*g* for 10 min at 4°C after standing at 4 °C for 30 min. For the bacterial fermentation products, 2 mL of each bacterial fermentation product was centrifuged at 12,000×*g* for 10 min at 4°C. The supernatant was collected, and the subsequent processing steps were consistent with those for the cecal content samples. The resulting supernatant was quantified using a gas chromatograph (Agilent 5975C GC system, Wilmington, NC, USA) after being filtered through a 0.22-μm membrane filter. The acetate, propionate, isobutyrate, butyrate, isovalerate, and valerate in the supernatant were determined.

RNA extraction, reverse transcription, and real-time qPCR

After collection, the tissues were immediately stored at − 80°C, and the cells were lysed by TRIzol (Invitrogen, CA, USA), and then stored at − 80°C. Before RNA extraction from bones, the bones were placed in ceramic crucibles and ground in liquid nitrogen. After grinding thoroughly, 0.1 g of powder was collected in 2 mL tubes containing 1 mL TRIzol.

For RNA extraction, 200 μL of chloroform was added to the lysates, and the samples were shaken and centrifuged at 12,000×*g* for 15 min at 4°C. For non-bone tissues, 500 μL of chloroform phase was collected, mixed with 500 μL of isopropanol, and centrifuged again as previously described. For bone tissues, 500 μL of the chloroform

phase was mixed with 500 μL of a mixed solution consisting of 0.8 mM sodium citrate and 1.2 mM sodium chloride. After standing at 4°C for 10 min, the resulting pellet was washed twice with 75% ethanol and ultimately resuspended in 20 μL of PCR-grade water.

A NanoDrop-2000 spectrophotometer (Thermo Scientific, MA, USA) was used to determine the purity and concentration of total RNA. Qualified RNA was subsequently used to synthesize cDNA with PrimeScript ™ RT reagent Kit with gDNA Eraser (RR047A, TaKaRa, Japan). Using cDNA as a template, qPCR was performed in a QuantStudio™ 7 Flex Real-Time PCR System (Applied Biosystems, CA, USA) using SYBR® Premix Ex TaqTM (RR420, TaKaRa, Japan) according to the manufacturer's guidelines. The primers used for the target genes in the present study are shown in Table S4. All samples were analyzed in triplicate. The results were analyzed using the $2^{-\Delta\Delta Ct}$ method, with β-actin serving as the reference.

Preparation of lymphocytes and flow cytometry

Single-cell suspensions of bone marrow were prepared as previously described [29]. Staining was performed for 30 min on ice in PBS containing 1% FBS. The antibodies used are listed in Table S5. Cells were acquired with a Coulter XL (Beckman Coulter, CA, USA), and analysis was performed with FlowJo and FCS Express 6 Flow software.

Measurement of eggshell quality

At weeks 20, 45, and 72, five eggs from each replicate (totaling 50 eggs per group) were randomly chosen for egg quality assessment. Egg quality was determined on three consecutive days, with egg collection conducted each day. Eggshell thickness was assessed using a vernier caliper. In brief, eggshell thickness was measured using a caliper. The measurements were taken from the upper, middle, and lower parts of the eggs after removing the inner membrane. The egg weight and breaking strength were determined by the Nabel DET-6000 egg analyzer (Kyoto, Japan). Eggshell strength was determined by measuring the maximum horizontal mechanical force experienced by the egg's long axis when it was laid flat.

Statistical analysis

Statistical analyses were conducted using SPSS version 20.0. The data are presented as the means ± standard deviations (SDs) unless indicated otherwise. The Shapiro–Wilk test was applied to assess the normality and lognormality of the data sets. Differences between the two groups were evaluated using a two-tailed unpaired Student's t-test. For data sets following a normal distribution and involving more than two groups, analysis was performed using one-way ANOVA, followed by Tukey's multiple comparisons test. For data not adhering to a normal distribution, the non-parametric Kruskal–Wallis test was utilized, followed by Dunn's multiple comparisons test. $P < 0.05$ was considered to indicate statistically significant.

Results

Age-related physiological changes in the femurs of laying hens

Age-related bone loss is a significant contributor to the deterioration of bone quality and microarchitecture, ultimately increasing fracture risk [44]. We hypothesized that changes in the bone microarchitecture of laying hens might be intricately linked to their egg-laying cycle. To investigate this possibility, we examined the femur microarchitecture at five pivotal age intervals (10, 25, 45, 72, and 98 weeks) (Fig. 2A). At 10 weeks, hens undergo a crucial developmental phase, not yet reaching sexual maturity. Between 25 and 45 weeks, hens are in their peak egg-laying period, achieving daily egg production rates as high as 95% [36]. A reduction in egg quantity and a decrease in eggshell quality are primary considerations for flock replacement in poultry farming by approximately 72 weeks [45]. Hens at 98 weeks represent the aged cohort.

Relative to that at 10 weeks, cortical bone volume (Cb. BV) significantly increased by 25 weeks and maintained stability up to 98 weeks (Fig. 2B). Cortical bone thickness

(See figure on next page.)

Fig. 2 Age-related physiological changes in the femur of laying hens. **A** Representative images of cortical bone (Cb), trabecular bone (Tb), and medullary bone (Mb) by micro-CT analysis. **B**–**E** Quantification of cortical bone volume (Cb. BV) (**B**), cortical bone thickness (Cb. Th) (**C**), cortical bone mineral density (Cb. BMD) (**D**), and cortical bone mineral content (Cb. BMC) (**E**). **F**–**J** Quantification of trabecular bone volume (BV) versus total femur volume ratio (Tb. BV/total volume [TV]) (**F**), trabecular bone thickness (Tb. Th) (**G**), trabecular bone surface area (BS) versus total femur volume ratio (Tb. BS/TV) (**H**), trabecular bone mineral content (Tb. BMC) (**I**), and trabecular bone mineral density (Tb. BMD) (**J**). **K** Quantification of the volume of the medullary cavity versus total femur volume ratio (BM. CV/TV). **L**–**N** Quantification of medullary bone volume versus total femur volume ratio (Mb. BV/TV) (**L**), medullary bone density (Mb. BMD) (**M**), and medullary bone mineral content (Mb. BMC) (**N**). **O** The mRNA expression of fibroblast growth factor 23 (FGF23). **P** Measurement of alkaline phosphatase (ALP) activity in the femur. **Q** Measurement of tartrate-resistant acid phosphatase (TRAP) activity in the femur. Data are shown as mean ± SD ($n = 12$–15 per group). Different letters on the scatter column chart represent significant differences ($P < 0.05$)

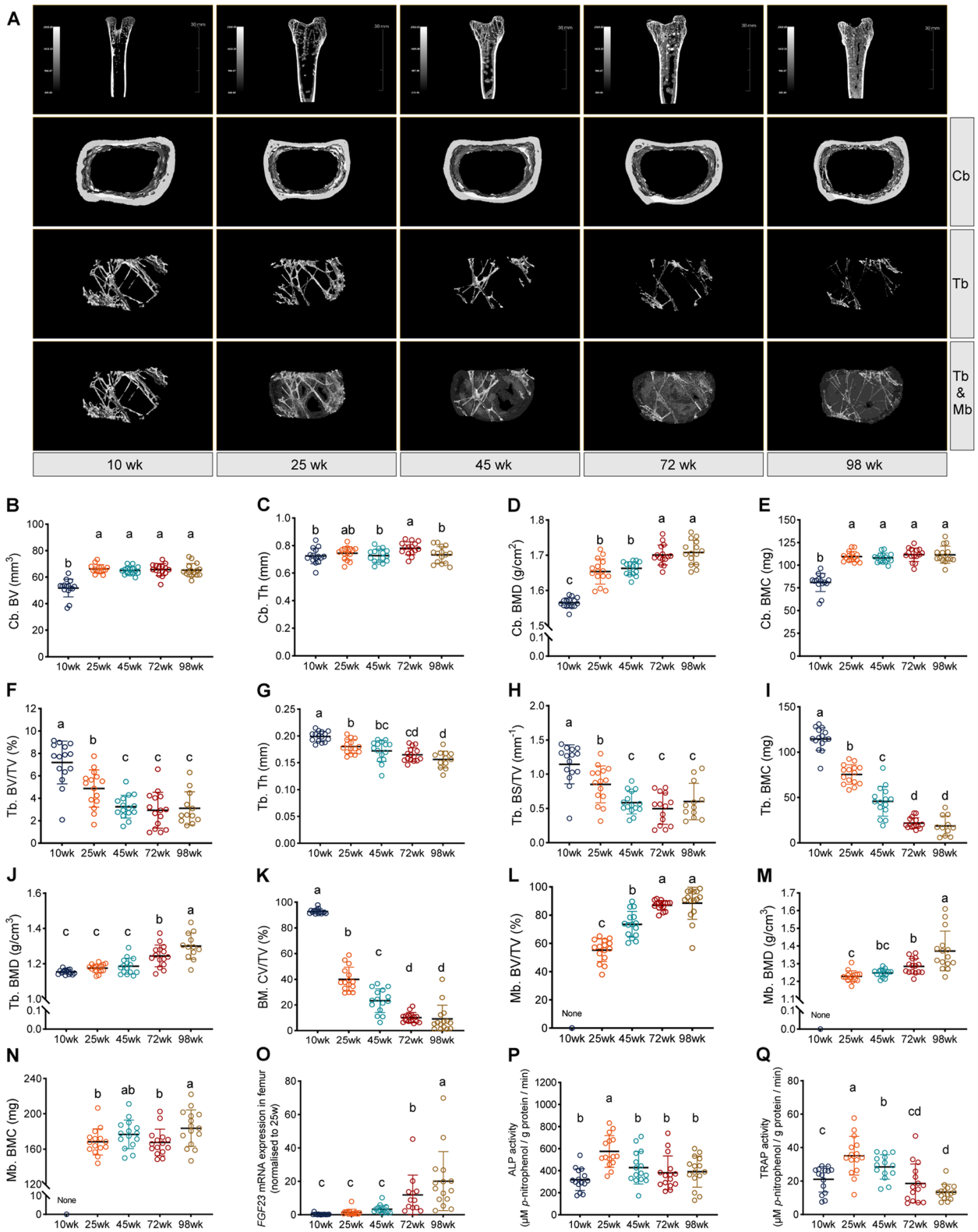

Fig. 2 (See legend on previous page.)

(Cb. Th) reached its zenith at 72 weeks, with negligible differences noted across other age groups (Fig. 2C). Cortical bone mineral density (Cb. BMD) exhibited a progressive increase with age, showing significantly greater density at 25 weeks and 45 weeks compared to 10 weeks and peaking at 72 weeks (Fig. 2D). The pattern for cortical bone mineral content (Cb. BMC) mirrored that of Cb. BV (Fig. 2E). Nonetheless, as laying hens aged, there was a marked decline in trabecular bone volume (Tb. BV), the ratio of Tb. BV to total femur volume (Tb. BV/TV), trabecular bone thickness (Tb. Th), trabecular bone surface area (Tb. BS), the ratio of Tb. BS to total femur volume (Tb. BS/TV), and the trabecular bone mineral content (Tb. BMC) (Fig. 2F–I, Fig. S1D and S1E). Following 25 weeks, the trabecular bone number (Tb. N) significantly decreased and stabilized through 98 weeks (Fig. S1G). Trabecular bone spacing (Tb. Sp) and connectivity density (Conn. D) displayed significant increases, with no notable change from 25 to 98 weeks (Fig. S1F and S1H). Trabecular bone mineral density (Tb. BMD) and trabecular bone pattern factor (Tb. Pf) increased after 45 weeks, significantly surpassing measurements at 10, 25, and 45 weeks (Fig. 2J and Fig. S1I). The degradation of trabecular bone microarchitecture has emerged as a defining feature of the onset of osteoporosis in mammals.

The ratio of the bone marrow cavity volume to the total femur volume (BM. CV/TV) diminished, reaching its nadir at 72 and 98 weeks (Fig. 2K), a phenomenon attributable to the progressive infilling of the medullary cavity by medullary bone. Concurrently, the medullary bone volume relative to the total femur volume (Mb. BV/TV) increased with age (Fig. 2L). From 25 to 98 weeks, both the medullary bone density (Mb. BMD) and medullary bone thickness (Mb. Th) exhibited a continuous increase (Fig. 2M and Fig. S1J). The medullary bone mineral content (Mb. BMC) reached its maximum at 98 weeks, with no significant variance noted among the other age groups (Fig. 2N). Fibroblast growth factor 23 (FGF23) plays a crucial role in the physiology of medullary bone, acting also as an inhibitor of osteogenic differentiation [41, 46]. Our analysis of *FGF23* mRNA expression in the femur revealed an age-associated increase (Fig. 2O). The medullary bone of laying hens manifests in two primary forms; it is absent before sexual maturity and initially emerges as a fine, loosely distributed structure around the trabecular bone upon reaching sexual maturity (Fig. 2A). With advancing age, the volume of medullary bone increased and consolidated into spherical structures, ultimately occupying the bone marrow cavity (Fig. S1B and S1C). Notably, in the 98-week cohort, three hens demonstrated this trait, with their bones completely devoid of a bone marrow cavity and exhibiting significantly enhanced hardness.

Alkaline phosphatase (ALP), a marker of osteoblast differentiation, and tartrate-resistant acid phosphatase (TRAP), indicative of osteoclastic resorption, were assessed in the femur. Both ALP and TRAP activities significantly increased from 10 to 25 weeks (Fig. 2P, Q), suggesting intensified bone remodeling to accommodate egg production demands. Post-25 weeks, ALP activity decreased, with no significant changes observed from 45 to 98 weeks, whereas TRAP activity significantly decreased from 25 to 98 weeks (Fig. 2P, Q).

Taken together, these findings indicate that aging does not precipitate osteoporosis in laying hens. Although the trabecular bone mass significantly decreases with age, the ongoing increase in the infill of medullary bone compensates for this decrease by enhancing overall bone hardness. Nonetheless, the age-related diminution in bone remodeling capability may impair laying performance, culminating in reduced egg quantity and quality.

Abundance and diversity changes of cecal microbiota across age

The succession of the gut microbiota is deeply intertwined with host physiology. To elucidate the interplay between the gut microbiota and bone in laying hens, we examined the developmental progression of microbial communities in the cecal contents from 10 to 98 weeks by 16S rRNA gene sequencing. The Shannon and Simpson indices for the cecal microbiota exhibited a marked increase from 10 to 45 weeks (Fig. 3A, B). Principal coordinate analysis (PCoA) revealed that the bacterial communities formed two distinct clusters delineating

(See figure on next page.)

Fig. 3 Abundance and diversity changes of cecal microbiota across age. Shannon index (**A**) and Simpson index (**B**) of the cecal microbiota. **C** Microbiota clustering based on a principal coordinate analysis (PCoA) of cecal microbiota. **D** Relative abundances of cecal microbiota at the genus level. **E** Clustered heatmap on the left shows the correlations between bacterial genera and the trabecular bone parameters (Tb. Pf, BMD, BMC, BV/TV, Th). Only significant correlations ($P < 0.05$) are shown. The color scale bar indicates the correlation coefficient (*r* value). The heatmap on the right shows the change in the relative abundance of bacteria at different ages. The color scale bar indicates the relative abundance standardized by z -score. F Clustered heatmap on the left shows the correlations between bacterial genera and the medullary bone parameters (Mb. BV/TV, BMD, BMC, Th). Only significant correlations ($P < 0.05$) are shown. The color scale bar indicates the correlation coefficient (*r* value). The heatmaps on the right show the changes in the relative abundance of bacteria at different ages. The color scale bar indicates the relative abundance standardized by z -score. Different letters on the scatter column chart represent significant differences ($P < 0.05$). $n = 15$ per group

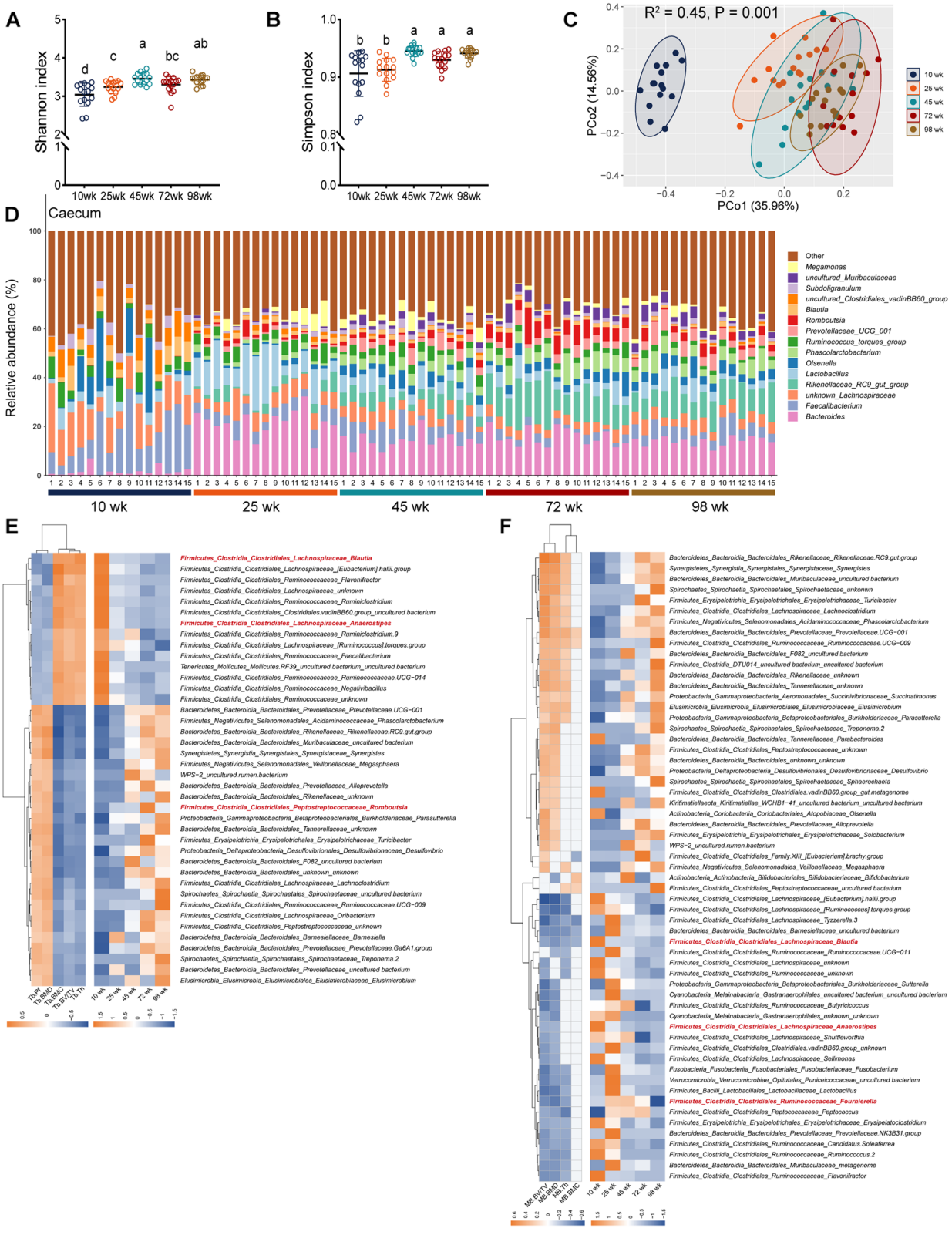

Fig. 3 (See legend on previous page.)

the pre- and post-sexual maturity stages. Furthermore, these bacterial community clusters varied significantly from 25 to 72 weeks ($R^2=0.45$; $P=0.001$, Fig. 3C), highlighting age as a pivotal determinant of microbial community structure, corroborated by changes in the relative abundance of genera (Fig. 3D). At 10 weeks, the microbial communities displayed low diversity, predominantly characterized by *Faecalibacterium* and an unidentified_*Lachnospiraceae*. By 25 weeks, there was a notable increase in the abundances of *Bacteroides* and *Lactobacillus*, concurrent with a decline in *Faecalibacterium*. With advancing age, the abundance of *Bacteroides* decreased, while that of *Rikenellaceae_RC9_gut_group* increased (Fig. 3D). Linear discriminant analysis (LDA) effect size (LEfSe) analysis further highlighted distinct differences in the cecal bacterial communities across ages (Fig. S2A).

To further explore the relationship between the cecal microbiota and bone development, we performed a correlation analysis linking the microbiota with trabecular bone and medullary bone parameters. Among the 14 bacterial genera showing a significant positive correlation with Tb. BMC, Tb. BV/TV, and Tb. Th, thirteen belonged to the class Clostridia ($P<0.05$, Fig. 3E). Importantly, most species within this class are capable of producing short-chain fatty acids (SCFAs), a bacterial metabolite critically linked to host health [28]. Conversely, the bacteria positively correlated with Tb. Pf and Tb. BMD originated from a more diverse array of classes ($P<0.05$, Fig. 3E). Among the twenty-seven bacterial genera demonstrating a significant negative correlation with Mb. BV/TV and medullary bone mineral density (Mb. BMD), seventeen were classified within Clostridia ($P<0.05$, Fig. 3F), suggesting divergent developmental trends between trabecular and medullary bone. Similarly, bacteria positively correlated with Mb. BV/TV and Mb. BMD originated from a varied background ($P<0.05$, Fig. 3E).

We noted that bacterial genera positively correlated with Tb. BMC, Tb. BV/TV, and Tb. Th were most prevalent at 10 weeks, whereas those negatively correlated with these parameters were more abundant at 72 and 98 weeks. Additionally, bacterial genera are positively associated with Mb. BV/TV and Mb. BMD showed greater abundance at 72 and 98 weeks. Consequently, we hypothesize that specific microbial populations may influence bone development at particular stages, highlighting the potential role of Clostridia species in the early phases of bone development.

Early exposure to specific strains regulates bone growth in chicks

Guided by our correlation analysis, we endeavored to identify specific strains within the microbiome with osteomodulatory potential. We pinpointed four genera—*Blautia, Fournierella, Anaerostipes,* and *Romboutsia*—associated with trabecular bone and medullary bone parameters, highlighted in red for emphasis (Fig. 3E, F, and Fig. S2A). Intriguingly, *Blautia* and *Anaerostipes* were more abundant at 10 weeks, *Fournierella* peaked at 45 weeks, and *Romboutsia* was predominant at 72 weeks (Fig. S2C–G). The abundances of *Blautia* and *Anaerostipes* were significantly positively correlated with Tb. BMC, Tb. BV/TV, and Tb. Th, yet negatively correlated with Mb. BV/TV, Mb. BMD, and Mb. Th (Fig. 3E, F). Conversely, *Romboutsia* showed a notable negative correlation with Tb. BMC, Tb. BV/TV, and Tb. Th (Fig. 3E), and the abundance of *Fournierella* was inversely related to Mb. BV/TV, Mb. BMD, and Mb. Th (Fig. 3F). By employing microbial culturomics, we isolated and identified specific strains from chicken intestines, namely *Blautia coccoides* CML164 (BC), *Fournierella sp002159185* CML151 (FS), *Anaerostipes caccae* CML199 (ANA), and *Romboutsia lituseburensis* CML137 (RL).

To further assess the influence of these strains on bone development, we inoculated them into chicks pretreated with an antibiotic cocktail and housed them in isolators. Fourteen days post-inoculation, none of the strains adversely impacted chick growth. Oral administration of ANA significantly promoted bone growth, as evidenced by an increase in femur length (Fig. 4A). Dual-energy X-ray absorptiometry (DEXA) analysis indicated that BC and ANA notably enhanced femoral BV, BMD, and BMC (Fig. 4C–E). Moreover, BC, FS, and ANA substantially increased femoral ALP activity (Fig. 4F), while only ANA promoted TRAP activity (Fig. 4G). The beneficial impact of BC and ANA on chick bone development reaffirms the positive association between the genera *Blautia* and *Anaerostipes* with Tb. BV. Collectively, these findings underscore the potential of early exposure to specific bacterial strains in regulating bone growth in chicks.

Effect of bacterial fermentation products on osteoblast mineralization

The gut microbiota communicates with distant organs via the production or induction of metabolites, hormones, neurotransmitters, and extracellular vesicles [23, 47, 48]. To elucidate the mechanisms through which BC and ANA enhance bone development, we exposed bone marrow mesenchymal stem cells (BMSCs) to bacterial fermentation products in Gifu anaerobic medium (GAM) during the induction of BMSCs differentiation into osteoblasts (Fig. 4H). Neither the blank GAM nor the fermentation products of BC influenced the mineralization of osteoblasts, as quantified by alizarin red S (ARS) staining (Fig. 4I, J). This observation suggested that BC may not directly

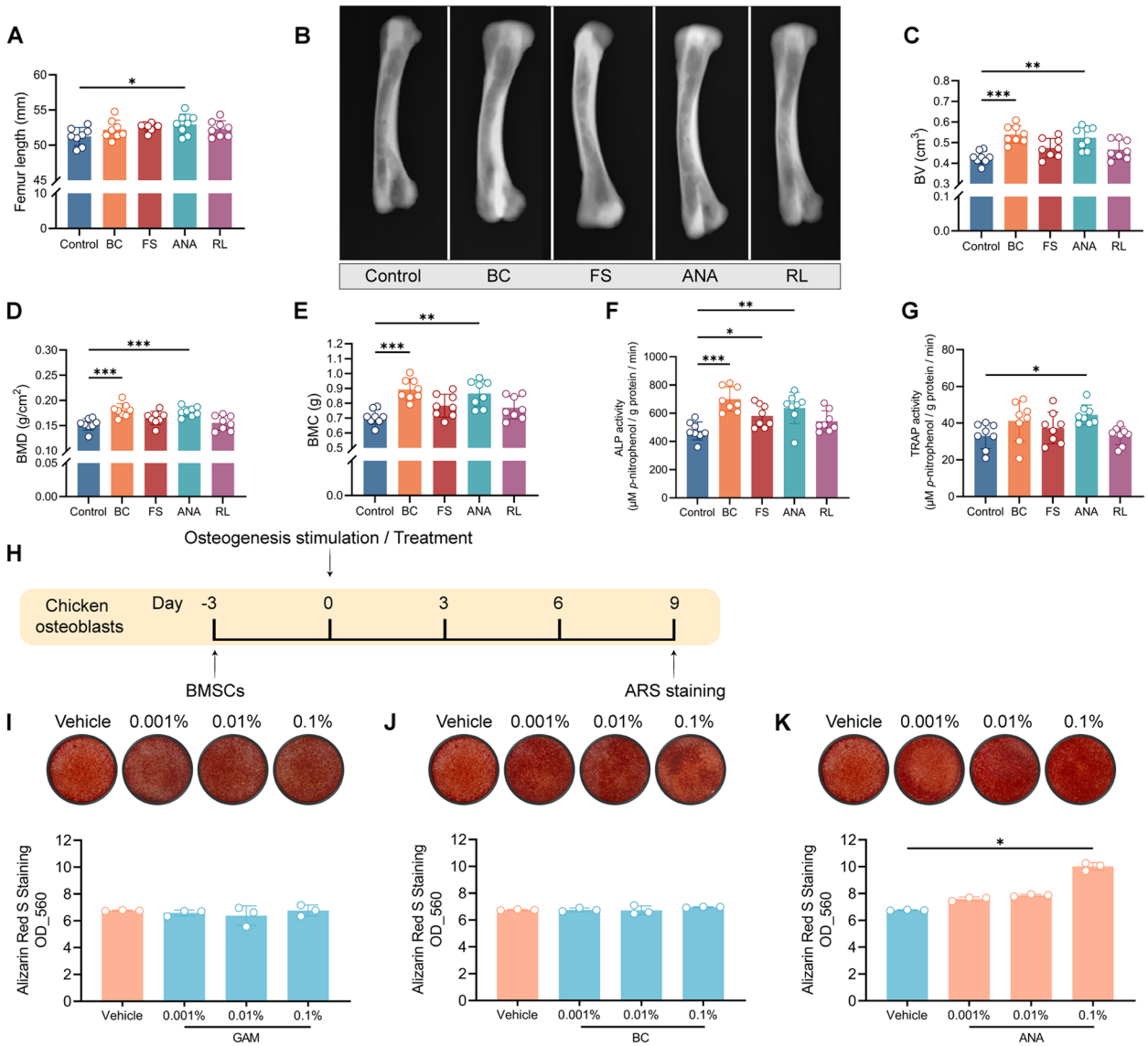

Fig. 4 Effect of specific strains or their metabolites on bone metabolism *in vitro* and *in vivo*. **A** Femur length in chicks inoculated with different bacterial strains. **B** Representative images of femurs obtained by dual-energy X-ray absorptiometry analysis (DEXA). **C**–**E** Quantification of DEXA showing the bone volume (BV) (**C**), bone mineral density (BMD) (**D**), and bone mineral content (BMC) (**E**) of the femur. **F** Measurement of alkaline phosphatase (ALP) activity in the femur. **G** Measurement of tartrate resistant acid phosphatase (TRAP) activity in the femur. $n = 8$ per group. **H** Schematic representation of the experiment *in vitro* experiment used to investigate the effect of metabolites from different strains on osteogenic mineralization. $n = 3$ per group. **I**–**K** Representative images and quantification of ARS staining in osteoblasts treated with blank GAM (**I**) or the fermentation products of BC (**J**) and ANA (**K**). Data are shown as mean ± SD. $^{*}P < 0.05$, $^{**}P < 0.01$, $^{***}P < 0.001$

modulate osteogenesis. In contrast, only 0.1% of the ANA fermentation products significantly promoted osteoblast mineralization (Fig. 4K). The promotive effects of ANA fermentation products on osteoblast mineralization corroborate the insights gained from correlation analysis. Although experiments at the strain level may not perfectly reflect the results of correlation analyses conducted at the genus level, the aforementioned findings indicate that specific constituents within ANA fermentation products contribute to the regulation of bone formation.

ANA promotes bone development by enhancing bone formation through butyrate

According to the results of the *in vivo* and *in vitro* assessments, ANA was the most potent enhancer of bone growth among the investigated strains. Notably, the oral administration of ANA over 14 days also led to an

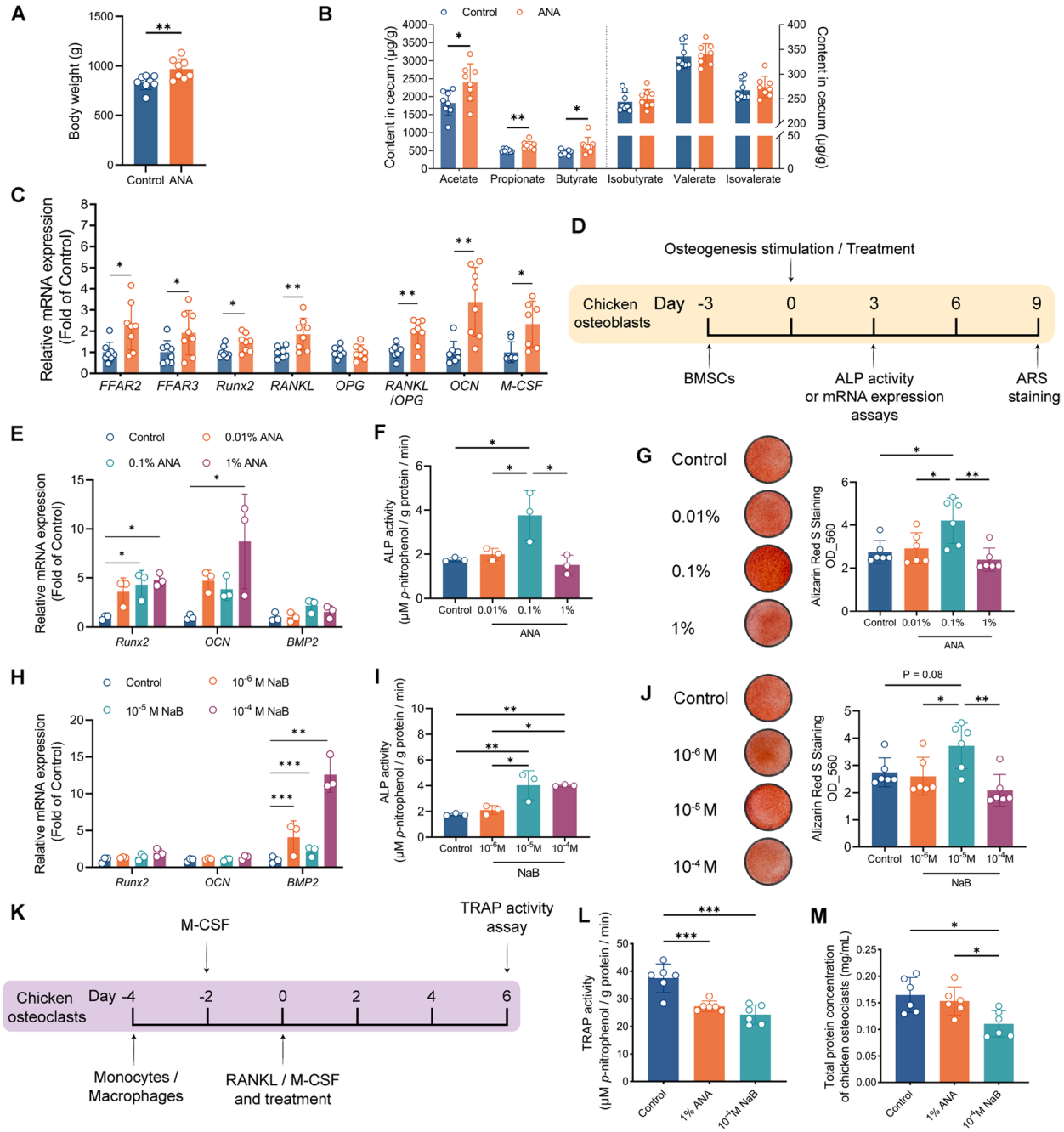

Fig. 5 ANA promotes bone development by enhancing bone formation through butyrate. **A**–**C** Measurement of the body weight of chicks (**A**), content of short-chain fatty acids (SCFAs) in cecal contents (**B**), and relative mRNA expression in the femur (**C**) after 14 days of inoculation. *n* = 7–8 per group. **D** Schematic representation of the experiment *in vitro* experiment used to investigate the effect of ANA fermentation products and NaB on osteogenesis in primary osteoblasts **E** The mRNA expression of runt-related transcription factor 2 (Runx2), osteocalcin (OCN), and bone morphogenetic protein 2 (BMP2) after supplementation with 0.01%, 0.1%, and 1% ANA fermentation products for 3 days. *n* = 3 per group. **F** ALP activity after supplementation with 0.01%, 0.1%, and 1% ANA fermentation products for 3 days. *n* = 3 per group. **G** Representative images and quantification of ARS staining after supplementation with 0.01%, 0.1%, and 1% ANA fermentation products for 9 days. *n* = 6 per group. **H** The mRNA expression of Runx2 , OCN, and BMP2 after 10 −6 M, 10 −5 M, or 10 −4 M NaB supplementation for 3 days. *n* = 3 per group. **I** ALP activity after 10 −6 M, 10 −5 M, or 10 −4 M NaB supplementation for 3 days. *n* = 3 per group. **J** Representative images and quantification of ARS staining after 10 −6 M, 10 −5 M, or 10 −4 M NaB supplementation for 9 days. *n* = 6 per group. **K** Schematic representation of the *in vitro* experiment used to investigate the effect of ANA or NaB on osteoclastogenesis in primary osteoclasts. *n* = 6 per group. **L**–**M** TRAP activity (**L**) and total protein concentration of osteoclasts (**M**) after administration of 1% ANA fermentation products or 10 −4 M NaB for 6 days. Data are shown as mean ± SD. * $P < 0.05$, ** $P < 0.01$, *** $P < 0.001$

increase in chicken body weight (Fig. 5A), prompting us to select ANA for a deeper exploration of its bone development promotion mechanisms in subsequent experiments.

ANA, first isolated from human feces in 2002, is a rod-shaped bacterium within the family *Lachnospiraceae* and genus *Anaerostipes* [49]. The genome map of ANA is depicted in Fig. S3. Species within *Lachnospiraceae* are known for their pronounced ability to produce SCFAs [50]. Initial analyses of SCFA content in cecal contents revealed that ANA inoculation significantly elevated the levels of acetate, propionate, and butyrate (Fig. 5B). Examination of SCFA receptors' mRNA expression in the femur indicated a substantial upregulation of free fatty acid receptor 2 (*FFAR2*) and free fatty acid receptor 3 (*FFAR3*). Furthermore, the expression of osteogenic-related mRNA, including runt-related transcription factor 2 (*Runx2*) and osteocalcin (*OCN*), along with osteoclastogenesis-related mRNA, such as receptor activator of nuclear factor kappa-B ligand (RANKL), the RANKL versus osteoprotegerin (*OPG*) ratio, and macrophage colony-stimulating factor (M-CSF), significantly increased post-ANA administration (Fig. 5C). These observations imply that the role of ANA in chick bone development may be mediated through SCFAs.

Further analysis of SCFAs in ANA fermentation products confirmed butyrate as its primary metabolite (Table S1). ANA fermentation products and sodium butyrate (NaB) were then applied during BMSCs differentiation into osteoblasts to evaluate their effects on osteogenesis (Fig. 5D). A 3-day induction with 0.1% ANA fermentation products upregulated *Runx2* mRNA expression, and 1% ANA products enhanced the expression of both *Runx2* and *OCN* (Fig. 5E). Only 0.1% ANA fermentation products increased ALP activity and osteoblast mineralization (Fig. 5F, G). At concentrations of 10^{-6} M, 10^{-5} M, and 10^{-4} M, NaB increased bone morphogenetic protein 2 (*BMP2*) mRNA expression, without significantly affecting *Runx2* and *OCN* (Fig. 5H). Both 10^{-5} M and 10^{-4} M NaB improved ALP activity (Fig. 5I), and 10^{-5} M NaB notably enhanced osteoblast mineralization after 9 days of treatment (Fig. 5J). These results suggest that butyrate is a critical element in the osteomodulatory effects of ANA.

To explore the impact of ANA metabolites and NaB on osteoclastogenesis, we supplemented primary chicken monocyte cultures with ANA metabolites and NaB during their differentiation into osteoclasts (Fig. 5K). After 6 days, 0.01% and 0.1% ANA, along with 10^{-6} M and 10^{-5} M NaB, did not affect TRAP activity or total protein concentration (data not shown). However, 1% ANA metabolites and 10^{-4} M NaB significantly inhibited TRAP activity (Fig. 5L), with ANA treatment not altering the total protein concentration, while NaB did (Fig. 5M). This finding suggested that ANA directly inhibits chicken primary osteoclast differentiation without affecting proliferation, whereas NaB inhibits both the proliferation and differentiation of osteoclasts. Nevertheless, previous research has indicated that butyrate concentrations in bone marrow may not be high enough to directly inhibit osteoclastogenesis *in vivo* [51], suggesting that ANA might not inhibit osteoclastogenesis *in vivo* through butyrate.

Dietary supplementation of ANA powder and coated sodium butyrate promotes bone development during sexual maturity

Postnatal bone development is crucial for sustaining overall health in animals. Previous studies have identified peak bone mass at skeletal maturity as a pivotal factor in preventing osteoporosis in humans [52]. In laying hens, bone health is intricately linked to egg production, particularly when they reach reproductive maturity and medullary bone begins to supply calcium for eggshell formation. During this critical phase, osteoclasts mobilize not only medullary bone but also trabecular and cortical bone. Insufficient bone development prior to sexual maturity could predispose laying hens to subsequent bone loss [53], underscoring the importance of comprehensive bone development for their health.

To evaluate the effect of ANA or butyrate on bone development during sexual maturity, laying hens were fed diets supplemented with ANA freeze-dried powder or with coated sodium butyrate (CSB) from 1 day of age to 20 weeks of age. Although the body weight of hens in the ANA group was initially slightly lower than that in the control group during the first 8 weeks, the body weight and shank length across all groups were equalized by week 20 (Fig. S4A–S4E). Dietary supplementation with ANA powder notably enhanced Cb. BV, Cb. Th, and Cb. BMC (Fig. 6B–D), without affecting Cb. BMD (Fig. 6E). Conversely, the impact of CSB on cortical bone development was less pronounced. In terms of trabecular bone parameters, ANA supplementation led to improvements in Tb. BV/TV, Tb. BV, Tb. BMD, and Tb. Th (Fig. 6F, H, J, and S4H). CSB supplementation significantly increased the Tb. BV/TV, Tb. BS/TV, and Tb. BS (Fig. 6F, G, and Fig. S4I). Notably, there were no significant differences in the Tb. N, Tb. Sp, Conn. D, and Tb. Pf among the three groups (Figure S4J–S4M). Compared with the ANA group, the CSB group had lower Tb. BMC, Tb. Th and BM. CV/TV (Fig. 6I, J, and Fig. S4G), which might be linked to differences in medullary bone development. Although ANA supplementation had no observable effect on medullary bone formation, CSB supplementation enhanced the Mb. BV/TV (Fig. 6K). Neither the

ANA nor the CSB treatments appeared to regulate Mb. BMC or Mb. BMD (Fig. 6L, M). This discrepancy in Mb. BV/TV might be attributed to variations in estradiol levels. Medullary bone formation in avians is closely associated with circulating estrogen [54, 55], and studies have indicated that inhibiting estrogen synthesis and its receptors before sexual maturity not only delays overall bone development but also impedes medullary bone formation [56]. Unlike ANA, CSB significantly elevated serum estradiol levels (Figure S4O).

Subsequent assessments of bone remodeling markers indicated that both ANA and CSB significantly enhanced femoral ALP activity and serum OCN levels (Fig. 6N, O). Femoral TRAP activity was not altered by either ANA or CSB (Fig. 6P), whereas CSB supplementation resulted in a reduction in serum C-terminal telopeptide of type I collagen (CTX-I) levels (Fig. 6Q). In conclusion, dietary supplementation with ANA and CSB facilitates bone development during sexual maturity in hens by promoting bone formation.

The skeletal and immune systems are closely interconnected [1, 57]. For instance, regulatory T cells (T-reg cells) positively influence bone formation by secreting anti-inflammatory cytokines, such as interleukin 10 (IL-10), and transforming growth factor-β (TGF-β) [1, 58, 59]. IL-10 enhances the secretion of OPG [60], and TGF-β is critical for the proliferation and early differentiation of osteoblast progenitor cells and matrix production [61]. T helper cell 17 (Th17) and tumor necrosis factor-alpha (TNF-α) positive cells, expressing M-CSF and RANKL, not only recruit inflammatory monocytes (osteoclast precursor cells) to the bone marrow, but also enhance osteoclastogenesis through increased production of interleukin 17 (IL-17), RANKL, and TNF-α [62, 63].

The development of immune cells following ANA and CSB treatment in the bone marrow was analyzed using flow cytometry, the gating strategy is illustrated in Figure S4P. Both ANA and CSB reduced the proportion of $CD3^+$ T cells, with CSB showing a significant decrease (Fig. 7A). The number of $CD4^+$ T cells was notably reduced after CSB treatment (Fig. 7B), whereas $CD8^+$ T cells remained unchanged after treatment with either ANA or CSB (Fig. 7C). Compared with that in the control group, the proportion of $CD25^+$ T cells (T-reg cells) significantly increased in both the ANA and CSB groups (Fig. 7D). $KuL01^+$ cells, representing monocytes/macrophages in the bone marrow, increased significantly in both groups (Fig. 7E). Similarly, $CD11c^+MHCII^+$ cells, denoting dendritic cells, were more prevalent in both the ANA and CSB groups than in the control group (Fig. 7F).

Furthermore, mRNA expression related to bone remodeling in the femur was analyzed. For SCFA receptors, CSB slightly elevated *FFAR2* expression (Fig. 7G). The expression of osteogenesis-related mRNA, including *Runx2* and *OCN*, as well as osteoclastogenesis-related mRNA, such as *RANKL* and *M-CSF*, was significantly upregulated following ANA and CSB administration. CSB notably increased *OPG* expression, while ANA exhibited a mild promotion (Fig. 7G). Regarding immune-related cytokines, ANA significantly upregulated *IL-10* mRNA expression, and both ANA and CSB increased *TGF-β* mRNA expression, consistent with the increase in $CD25^+$ T cells (Fig. 7D, G). Moreover, *IL-17* mRNA expression was elevated in both the ANA and CSB groups, with ANA showing the most significant upregulation (Fig. 7G). Thus, we propose that ANA and CSB may improve the bone marrow niche by increasing specific immune cell populations during sexual maturation.

Continuous dietary supplementation of ANA powder prevents age-induced bone loss

As hens entered the active laying phase, we divided the ANA group into two subgroups to assess the durability of the effects of ANA on bone health. One subgroup, labeled continuous ANA (cANA), maintained ANA powder supplementation in their diet, whereas the second subgroup, termed stopped ANA (sANA), ceased receiving ANA powder. This bifurcation aimed to determine whether the enhanced bone mass acquired during sexual maturity could mitigate future bone loss and examine the enduring impact of ANA supplementation on bone physiology.

(See figure on next page.)

Fig. 6 Dietary supplementation of ANA powder and coated sodium butyrate promotes bone development during sexual maturity. **A** Micro-CT images of cortical bone (Cb), trabecular bone (Tb), and medullary bone (Mb) in femurs from control group, ANA group (dietary supplementation of Anaerostipes caccae CML199 powder), and CSB group (dietary supplementation of coated sodium butyrate). **B**–**E** Quantification of cortical bone volume (Cb. BV) (**B**), cortical bone thickness (Cb. Th) (**C**), cortical bone mineral content (Cb. BMC) (**D**), and cortical bone mineral density (Cb. BMD) (**E**). **F**–**J** Quantification of the trabecular bone BV/TV (Tb. BV/TV) (**F**), trabecular bone BS/TV (Tb. BS/TV) (**G**), trabecular bone mineral density (Tb. BMD) (**H**), trabecular bone mineral content (Tb. BMC) (**I**), and trabecular bone thickness (Tb. Th) (**J**). **K–M** Quantification of the medullary bone BV/TV (Mb. BV/TV) (**K**), medullary bone mineral content (Mb. BMC) (**L**), and medullary bone density (Mb. BMD) (**M**). **N**–**Q** Measurement of alkaline phosphatase (ALP) activity in the femur (**N**), serum osteocalcin (OCN) (**O**), tartrate resistant acid phosphatase (TRAP) activity in the femur (**P**), and serum C-terminal telopeptide-I (CTX-I) (**Q**). Data are shown as mean ± SD ($n = 9$–10 per group). * $P < 0.05$, ** $P < 0.01$, *** $P < 0.001$

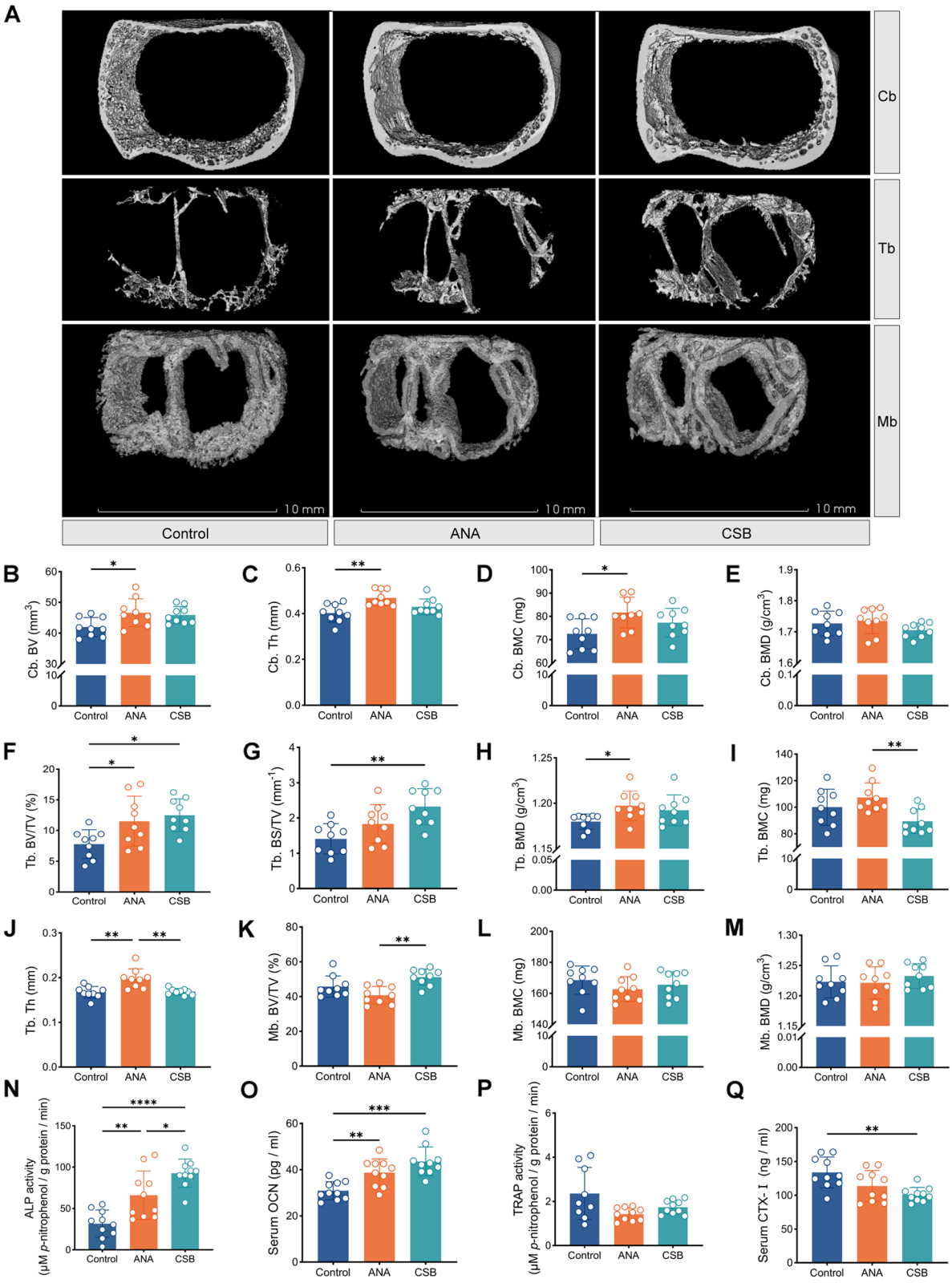

Fig. 6 (See legend on previous page.)

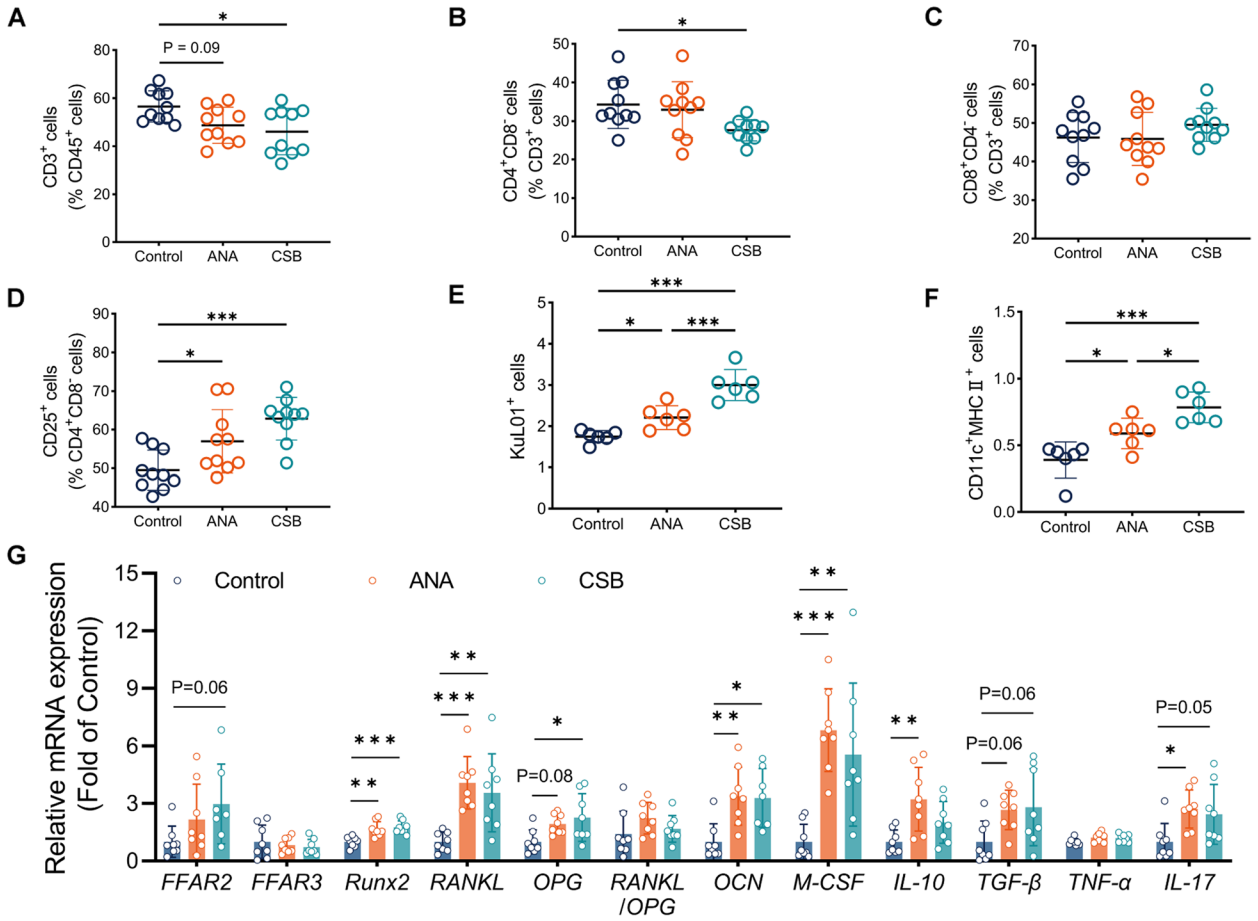

Fig. 7 Effect of ANA powder and CSB on immune cells associated with bone remodeling in bone marrow. **A**–**F** The proportions of immune-related cells in the bone marrow of laying hens in the control group, ANA group (dietary supplementation of Anaerostipes caccae CML199 powder), and CSB group (dietary supplementation of coated sodium butyrate). $n = 6$–10 per group. **G** mRNA expression associated with bone remodeling in the femur. $n = 7$–8 per group

Our analysis revealed that both the cANA and sANA subgroups experienced a slight increase in Cb. Th while exhibiting a significant reduction in Cb. BMD, with the cANA showing a more substantial decrease in BMD (Fig. 8C, D). Notably, cANA displayed a considerable protective effect on Tb. BV/TV, Tb. BS/TV, Tb. Th, Tb. BV, Tb. BS, and Conn.D (Fig. 8F, G, J, Fig. S5D, S5E, and S5H). This was paired with a minor decline in Tb. BMD and a significant reduction in Tb. Pf (Fig. 8H and Fig. S5I). The bone parameters of the sANA group were an intermediary between those of the cANA and control groups, indicating a moderate effect (Fig. 8F–J, Fig.

(See figure on next page.)

Fig. 8 Continuous dietary supplementation of ANA powder prevents age-induced bone loss. **A** Representative images of cortical bone (Cb), trabecular bone (Tb), and medullary bone (Mb) in the femur by Micro-CT analysis in the control group, cANA group (continuous dietary supplementation ANA powder), and sANA group (stopped receiving dietary supplementation of ANA powder). **B**–**E** Quantification of cortical bone volume (Cb. BV) (**B**), cortical bone thickness (Cb. Th) (**C**), cortical bone mineral density (Cb. BMD) (**D**), and cortical bone mineral content (Cb. BMC) (**E**). **F**–**J** Quantification of the trabecular bone BV/TV (Tb. BV/TV) (**F**), trabecular bone BS/TV (Tb. BS/TV) (**G**), trabecular bone mineral density (Tb. BMD) (**H**), trabecular bone mineral content (Tb. BMC) (**I**), and trabecular bone thickness (Tb. Th) (**J**). **K**–**M** Quantification of the medullary bone BV/TV (**K**), medullary bone density (Mb. BMD) (**L**), and medullary bone mineral content (Mb. BMC) (**M**). **N**–**Q** Measurement of alkaline phosphatase (ALP) activity in the femur (**N**), serum osteocalcin (OCN) (**O**), tartrate resistant acid phosphatase (TRAP) activity in the femur (**P**), and serum C-terminal telopeptide-I (CTX-I) (**Q**). **R** Differences in the bacterial communities at the genus level were tested by linear discriminant analysis effect size, with a linear discriminant analysis (LDA) score > 2 and $P < 0.05$. $n = 8$ per group. **S** Measurement of the content of short-chain fatty acids (SCFAs) in cecal contents. Data are shown as mean ± SD ($n = 10$ per group). * $P < 0.05$, ** $P < 0.01$, *** $P < 0.001$

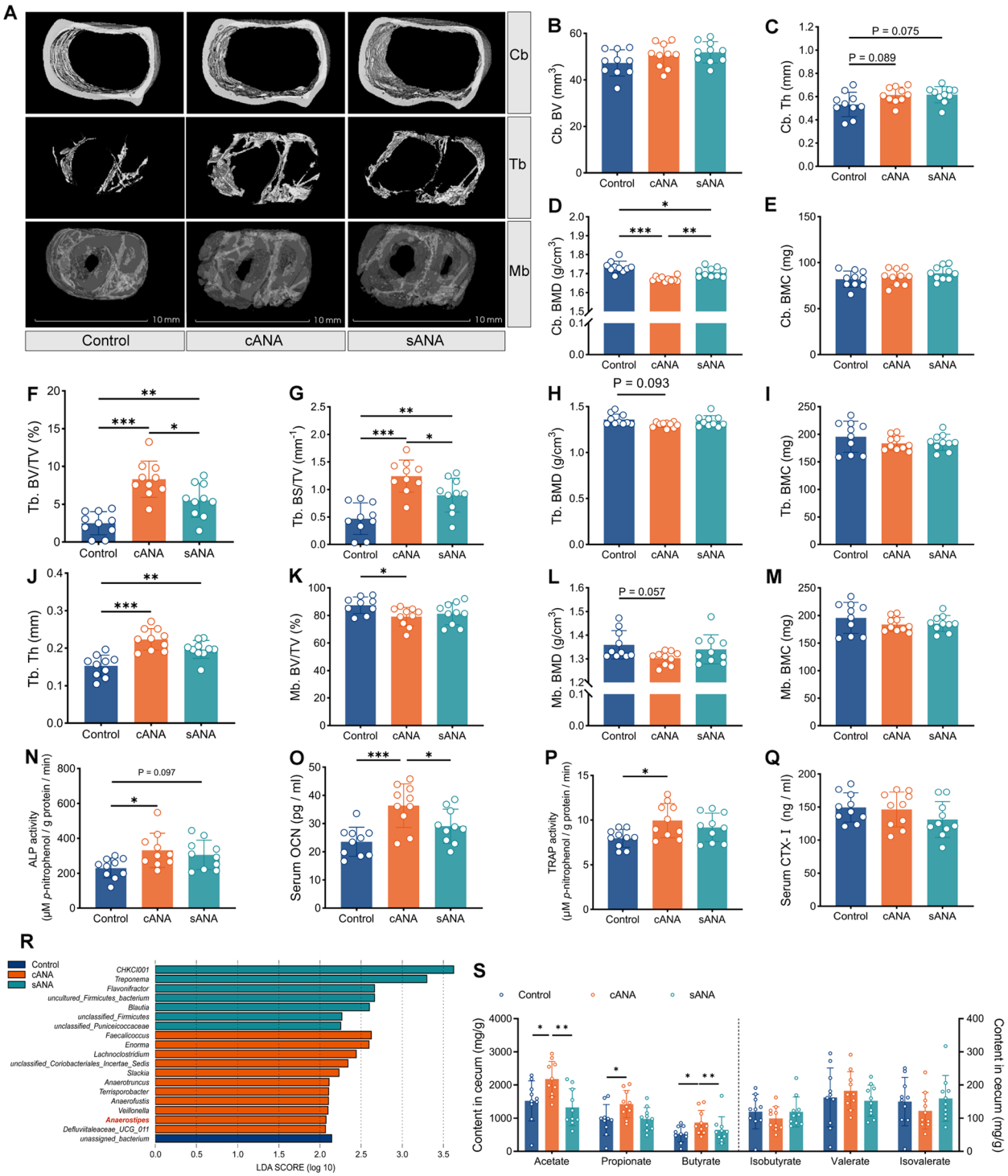

Fig. 8 (See legend on previous page.)

S5D–S5I). In the cANA group, Mb. BV/TV was significantly lower compared to the control group, alongside a slight reduction in Mb. BMD and no significant changes in Mb. BMC and Mb. Th (Fig. 8K–8M and Fig. S5J). Interestingly, the control group showed a tendency for the medullary bone to form spherical structures or fill the bone marrow cavity (Fig. S5A and S5B). These outcomes suggest that the accrued bone mass during sexual

maturity could delay the degradation of both cortical and trabecular bone. Continuous dietary supplementation with ANA powder effectively enhanced the microarchitectural quality of cortical and trabecular bone, thus preventing an excessive increase in Mb. BV/TV and maintaining overall femoral bone density. Concerning bone remodeling markers, femoral ALP activity, serum OCN levels, and femoral TRAP activity in the cANA group were significantly elevated compared to those in the control group, while sANA slightly increased femoral ALP activity only (Fig. 8N–Q), indicating more active bone remodeling within the cANA group. Following the cessation of ANA powder supplementation, serum estradiol levels significantly increased (Fig. S5K). Despite this increase, there was no significant enhancement in Mb. BV/TV. Therefore, we speculate that alterations in estrogen levels in older hens do not markedly affect medullary bone microarchitecture.

Continuous dietary supplementation of ANA powder enhances the colonization of Anaerostipes and cecal SCFA production

To evaluate the impact of cANA and sANA supplementation of ANA powder on the cecal microenvironment, we conducted 16S rRNA sequencing and assessed the production of SCFAs in cecal content. No significant alterations were observed in the Shannon or Simpson indices (Fig. S5L and S5M), and PCoA confirmed similar microbial diversity across the groups (Fig. S5N). *Bacteroides* emerged as the genus with the highest relative abundance across all groups (Fig. S5O). LEfse analysis indicated that cANA had a more enriched differential profile, notably including *Anaerostipes* (Fig. 8R). Analysis of cecal SCFAs showed significantly increased levels of acetate, propionate, and butyrate in the cANA group compared to both the sANA and control groups (Fig. 8S). These findings suggest that continuous ANA supplementation not only promotes the colonization of *Anaerostipes* but also boosts the capacity of the cecal microbiota for SCFA production. This finding reaffirms the pivotal role of SCFAs in mediating gut-bone axis communication in laying hens, highlighting the beneficial effects of sustained ANA intake.

The physiological state of laying hen bones is related to the eggshell quality

In the poultry industry, a harder eggshell can significantly reduce the risk of breakage during transportation. Aging in laying hens often leads to diminished eggshell quality. Considering the close connection between the skeletal system of laying hens and egg production, we evaluated eggshell quality at 20, 45, and 72 weeks to investigate the correlation between bone physiology and eggshell quality. The findings revealed that the enhancement of bone development by ANA and CSB supplementation contributed to improved eggshell strength (Fig. S6A). Notably, at 45 and 72 weeks, eggshell thickness was greatest in the cANA group (Fig. S6B and S6C). Thus, during the peak egg-laying period, increased bone mass and more dynamic bone remodeling are associated with greater eggshell formation. In the later stages of egg production, the reduced medullary bone volume and intensified bone remodeling observed in the cANA group may have enhanced the mobilization of bone calcium, supporting the synthesis of eggshells in laying hens.

Discussion

The role of the gut microbiota in regulating bone development was first reported in mice in 2012 [14]. Since this groundbreaking discovery, numerous studies have advanced our understanding of gut–bone communication, from artificial microbiota interventions to the impact of specific bacterial strains. Our previous review provides a comprehensive overview of these studies [5]. This research offers novel insights into key aspects of the gut-bone axis. Initially, we explored the relationship between bone development patterns and dynamic changes in the cecal microbiota of laying hens, highlighting the potential role of certain Clostridia genera in postnatal bone development. Subsequently, we identified and validated a symbiotic bacterium from the chicken gut, ANA, for its osteomodulatory effects mediated by butyrate, both *in vivo* and *in vitro*. ANA not only facilitated postnatal bone development but also countered age-induced trabecular bone loss.

Given the impact of sustained high egg production on bone health due to extended calcium mobilization, laying hens serve as an ideal model for investigating the interplay between bone metabolism and gut microbiota [36]. We selected five representative ages to examine their bone microarchitecture throughout maturation and aging. Significant changes in cortical bone were observed pre- and post-sexual maturity, underscoring the importance of early life stages in bone growth. The volume and thickness of trabecular bone decreased with age in laying hens, mirroring osteoporotic phenotypes seen in mammals. Unlike mammals, laying hens have fewer Tb. N and an expanded medullary cavity, possibly representing an evolutionary adaptation for flight. Bone mineral density is a vital, non-invasive measure of bone strength in humans [10], yet it shows a peculiar trend in laying hens. Contrary to the well-documented decline in bone density and elasticity with age in mammals [9], laying hens show an increase in both cortical and trabecular bone density with age, a phenomenon noted in previous research [64]. This distinctive age-related pattern in laying hens

warrants further investigation to elucidate the underlying mechanisms involved.

Medullary bone is prevalent across avian species within the orders Galliformes (including chickens and quails), Anseriformes (ducks and other waterfowl), Columbiformes (pigeons), and Passeriformes (such as house finches and pine siskins) [55, 65]. Estrogen levels are crucial for medullary bone formation [56]. Dietary supplementation with NaB has been shown to elevate serum estradiol levels in 20-week-old hens, leading to an increased volume of medullary bone. Initially, at the onset of sexual maturity, the medullary bone mass is minimal, encasing the trabecular bone. As hens age, the volume of medullary bone expands, peaking at 72 weeks. This growth is accompanied by a transition from a diffuse to a more concentrated spherical distribution, ultimately occupying the bone marrow cavity. It is hypothesized that medullary bone volume inversely affects laying performance, where a smaller volume indicates more active bone remodeling, facilitating efficient medullary bone absorption by osteoclasts. Conversely, a larger volume implies a more complex absorption process. Moreover, the activity of characteristic enzymes of osteoblasts and osteoclasts in the femur decreases with age in laying hens, suggesting a reduction in bone remodeling efficiency. Contrary to the process observed in mammals, laying hens do not experience osteoporosis with aging. Despite the gradual loss of trabeculae, the presence of abundant medullary bone compensates by providing mechanical strength, with both the average elastic modulus and hardness increasing with age [66]. This observation is consistent with findings that a higher rate of medullary bone filling is associated with increased bone-breaking strength [34]. However, this advantage comes at the cost of reduced egg production quantity and quality in older laying hens.

Correlation analysis preliminarily indicated that the cecal microbiota is linked to the bone development of laying hens. A notable positive relationship was observed between the class Clostridia and Tb. BV/TV and Tb. Th with the relative abundance of Clostridia peaking at 10 weeks and diminishing with age. Consequently, we propose that certain Clostridia species are integral to early bone development. Although leveraging the gut microbiota as a biomarker for osteoporosis is subject to debate [67], correlation analysis offers a novel method for identifying specific strains or probiotics with potential health benefits.

Probiotics, defined as "live microorganisms that confer a health benefit on the host when administered in adequate amounts" [68], were also a focus of this study, aiming to uncover the next generation of probiotics with osteomodulatory properties. Through correlation and LEfse analyses, we identified four strains from the chicken intestine. ANA and BC were notable for their significant positive effects on chick bone development, without adverse side effects. ANA also contributed to an increase in femur length. Only ANA metabolites enhanced osteoblast mineralization *in vitro*, whereas BC metabolites did not exhibit a similar effect, suggesting that the osteogenic promotion of ANA may be attributed to its metabolites, with butyrate identified as a pivotal factor in osteogenic differentiation. A 14-day oral administration of ANA led to a significant increase in butyrate levels in chicken cecal contents. Furthermore, the increase in femoral ALP and TRAP activities post-ANA inoculation indicates that ANA may facilitate bone remodeling through butyrate, enhancing bone development. ANA fermentation products have been shown to promote osteogenesis and inhibit osteoclastogenesis *in vitro*. While SCFAs impede osteoclast differentiation *in vitro*, their direct regulation of osteoclastogenesis *in vivo* remains uncertain [51]. The complex milieu of the bone marrow niche involves multiple factors influencing osteoclast differentiation, which are not fully replicable in *in vitro* assays.

SCFAs, key regulatory metabolites produced by the gut microbiota, including acetate, propionate, and butyrate, play a pivotal role across the skeletal system [69]. They impact satellite cell homeostasis and skeletal muscle development and offer relief in conditions such as arthritis and osteoporosis [28, 70, 71]. Our findings, alongside previous research, underscore the significant effect of butyrate on bone formation [28, 72, 73]. Consequently, factors affecting SCFA levels, such as adherence to a Mediterranean diet, are crucial for improving bone health [74, 75]. Furthermore, investigating microbial strains that enhance SCFA production, particularly those within the *Lachnospiraceae* family, could deepen our understanding of their role in bone health. Notably, ANA has been associated with health benefits, including mitigating milk allergy reactions and inhibiting colorectal tumors in mice [76, 77]. Additionally, a lower abundance of *Anaerostipes* has been observed in Chinese osteoporosis patients compared to the general population [67]. Our study adds to the body of evidence supporting the osteomodulatory capacity of ANA.

Most research on the impact of gut microbiota on bone health has focused on its potential to mitigate osteoporosis in ovariectomized mouse models. It is equally imperative to explore whether bacteria can enhance bone mass accumulation during an animal's puberty under physiological conditions. This investigation examined the effects of ANA and butyrate on chicken bone development in a standard rearing environment and revealed that both ANA and CSB promote bone development during the sexual maturity of laying hens, with

ANA exhibiting superior efficacy. Interestingly, the body weight of chickens in the ANA group was slightly lower than that in the control group before 16 weeks, suggesting a potential prioritization of skeletal over general body growth. By 20 weeks, ANA had no significant impact on estradiol levels, nor did it significantly alter the microarchitecture of medullary bone, indicating that ANA facilitates structural bone development without compromising medullary bone integrity or causing adverse effects. Dietary supplementation with ANA and CSB also improved the bone marrow niche by increasing immune cell populations associated with bone remodeling and supporting bone development during sexual maturation by upregulating genes related to bone remodeling. As a result, the improvement of ANA and CSB on bone physiology helps to increase eggshell quality during the active laying phase.

Aging-induced bone loss significantly contributes to osteoporosis [9]. Between 20 to 72 weeks, we subdivided the ANA group into two groups: the cANA group and the sANA group. The cANA subgroup sustained higher bone mass and exhibited more active bone remodeling compared to other groups. The sANA subgroup showed that accumulated bone mass during sexual maturity could postpone trabecular bone loss. Interestingly, chicken femur bone density tended to increase with age, although the underlying causes have yet to be elucidated. Continuous feeding of ANA powder seemed to attenuate the increasing trend of cortical bone, trabecular bone, and medullary bone mineral density. Despite a reduction in serum estradiol levels at 72 weeks compared to 20 weeks, the levels remained relatively elevated. The sANA group had the highest estradiol levels, yet no significant correlation was found between estrogen and medullary bone at this age. A significant shift was observed in the cecal niche at 72 weeks. The cANA significantly enhanced the abundance of the genus *Anaerostipes*, which was accompanied by the highest level of SCFAs. cANA also contributed to ongoing eggshell quality improvements, potentially decreasing breakage risks during transportation. The cANA group showcases elevated bone remodeling markers and lower Mb. BV/TV compared to other groups, may enable more efficient mobilization of bone calcium for eggshell synthesis.

Conclusion

This investigation elucidated the unique bone developmental patterns of laying hens and identified a new probiotic strain with osteomodulatory effects. Our results underscore that the continuous deposition of medullary bone in the bone marrow cavity leads to significant trabecular bone loss as laying hens age. The cecal microbial composition significantly shifted before and after sexual maturity, with some genera within the class Clostridia potentially linked to postnatal bone development in laying hens. ANA demonstrated the most significant promotion of bone formation both *in vivo* and *in vitro* through butyrate in its fermentation products. ANA enhances bone development during sexual maturity by improving the immune microenvironment of the bone marrow in laying hens. Continuous dietary supplementation of ANA for 50 weeks prevented excessive medullary bone deposition and mitigated aging-induced trabecular bone loss. This study lays the groundwork for future explorations into microbial-based interventions, potentially opening new avenues for the prevention and treatment of bone-related disorders in both poultry and possibly extending to human health, emphasizing the close connections within the gut-bone axis.

Abbreviations

ALP	Alkaline phosphatase
ANA	*Anaerostipes caccae* CML199
ARS	Alizarin red S
BC	*Blautia coccoides* CML164
BM. CV/TV	The bone marrow cavity volume to the total femur volume
BMP2	Bone morphogenetic protein 2
BMSCs	Bone marrow mesenchymal stem cells
cANA	Continuous ANA powder supplementation in the conventional diet
Cb	Cortical bone
Cb. BMC	Cortical bone mineral content
Cb. BMD	Cortical bone mineral density
Cb. BV	Cortical bone volume
Cb. Th	Cortical bone thickness
Conn. D	Connectivity density
CSB	Coated sodium butyrate
CTX-I	C-terminal telopeptide of type I collagen
DEXA	Dual-energy X-ray absorptiometry
DMEM	Dulbecco's modified Eagle's medium
FBS	Fetal bovine serum
FFAR2	Free fatty acid receptor 2
FFAR3	Free fatty acid receptor 3
FGF23	Fibroblast growth factor 23
FS	*Fournierella sp002159185* CML151
GAM	Gifu anaerobic medium
IL	Interleukin
LEfSe	Linear discriminant analysis effect size
Mb	Medullary bone
Mb. BMC	Medullary bone mineral content
Mb. BMD	Medullary bone mineral density
Mb. BS/TV	The ratio of Mb. BS to total femur volume
Mb. BS	The medullary bone surface area
Mb. BV/TV	The ratio of medullary bone volume to total femur volume
Mb. BV	Medullary bone volume
Mb. Th	Medullary bone thickness
M-CSF	Macrophage colony-stimulating factor
NaB	Sodium butyrate
OCN	Osteocalcin
OPG	Osteoprotegerin
PCoA	Principal coordinate analysis
RANKL	Receptor activator of nuclear factor kappa-B ligand
RL	*Romboutsia lituseburensis* CML137
Runx2	Runt-related transcription factor 2
sANA	Discontinuation of ANA powder supplementation in the conventional diet
SCFAs	Short-chain fatty acids
Tb	Trabecular bone

Tb. BMC	Trabecular bone mineral content
Tb. BMD	Trabecular bone mineral density
Tb. BS/TV	The ratio of trabecular bone surface area to total femur volume
Tb. BS	Trabecular bone surface area
Tb. BV/TV	The ratio of trabecular bone volume to total femur volume
Tb. BV	Trabecular bone volume
Tb. N	Trabecular bone number
Tb. Pf	Trabecular bone pattern factor
Tb. Sp	Trabecular bone spacing
Tb. Th	Trabecular bone thickness
TGF-β	Transforming growth factor-β
Th17	T helper cells 17
TNF-α	Tumor necrosis factor-alpha
TRAP	Tartrate-resistant acid phosphatase
T-reg cells	Regulatory T cells
VOI	Volume of interest
wk	Weeks

Supplementary Information

The online version contains supplementary material available at https://doi.org/10.1186/s40168-024-01920-y.

Supplementary Material 1.

Acknowledgements
We appreciated Sichuan Sundaily Farm Ecological Food Co., Ltd. for animal feeding.

Authors' contributions
YG and DL designed the project. ZL carried out the experimental work, bioinformatic analyses, and drafted the manuscript. GY, YZ, FZ, YL, YFL, GL, YW, and MZ collected samples. All the other authors revised and edited the manuscript. All authors read and approved the final manuscript.

Funding
This work was supported by the National Key Research and Development Program of China (2022YFD1300400) and the 2115 Talent Development Program of China Agricultural University.

Data availability
The genome data have been deposited in NCBI BioProject PRJNA1076119. The rest of the raw datasets are available on FigShare (https://figshare.com/articles/dataset/data1_xlsx/25231592. Accessed 2 February 2024).

Declarations

Ethics approval and consent to participate
All the experiments were reviewed and approved by the Institutional Animal Care and Use Committee of China Agricultural University (statement no. AW10204202-1–3).

Consent for publication
Not applicable.

Competing interests
The authors declare no competing interests.

Author details
[1]State Key Laboratory of Animal Nutrition and Feeding, College of Animal Science and Technology, China Agricultural University, Beijing 100193, China. [2]Animal Nutrition Institute, Sichuan Agricultural University, Chengdu, Sichuan 611130, China. [3]Sichuan Tieqilishi Industrial Co., Ltd, Mianyang 621010, China.

Received: 29 April 2024 Accepted: 28 August 2024
Published online: 22 October 2024

References

1. Okamoto K, Nakashima T, Shinohara M, Negishi-Koga T, Komatsu N, Terashima A, et al. Osteoimmunology: the conceptual framework unifying the immune and skeletal systems. Physiol Rev. 2017;97(4):1295–349. https://doi.org/10.1152/physrev.00036.2016.
2. Tsukasaki M, Takayanagi H. Osteoimmunology: evolving concepts in bone-immune interactions in health and disease. Nat Rev Immunol. 2019;19(10):626–42. https://doi.org/10.1038/s41577-019-0178-8.
3. Florencio-Silva R, Sasso GR, Sasso-Cerri E, Simões MJ, Cerri PS. Biology of bone tissue: structure, function, and factors that influence bone cells. Biomed Res Int. 2015. https://doi.org/10.1155/2015/421746.
4. Zhou R, Guo Q, Xiao Y, Guo Q, Huang Y, Li C, et al. Endocrine role of bone in the regulation of energy metabolism. Bone Res. 2021;9(1):25. https://doi.org/10.1038/s41413-021-00142-4.
5. Lyu Z, Hu Y, Guo Y, Liu D. Modulation of bone remodeling by the gut microbiota: a new therapy for osteoporosis. Bone Res. 2023;11(1):31. https://doi.org/10.1038/s41413-023-00264-x.
6. Hadjidakis DJ. Androulakis, II, one remodeling. Ann N Y Acad Sci. 2006;1092:385–96. https://doi.org/10.1196/annals.1365.035.
7. Chan GK, Duque G. Age-related bone loss: old bone, new facts. Gerontology. 2002. https://doi.org/10.1159/000048929.
8. Nagaraja S, Lin AS, Guldberg RE. Age-related changes in trabecular bone microdamage initiation. Bone. 2007. https://doi.org/10.1016/j.bone.2006.10.028.
9. Kavukcuoglu NB, Denhardt DT, Guzelsu N, Mann AB. Osteopontin deficiency and aging on nanomechanics of mouse bone. J Biomed Mater Res A. 2007. https://doi.org/10.1002/jbm.a.31081.
10. Sambrook P, Cooper C. Osteoporosis. Lancet. 2006. https://doi.org/10.1016/s0140-6736(06)68891-0.
11. Khosla S, Hofbauer LC. Osteoporosis treatment: recent developments and ongoing challenges. Lancet Diabetes Endocrinol. 2017. https://doi.org/10.1016/s2213-8587(17)30188-2.
12. Wei H, Xu Y, Wang Y, Xu L, Mo C, Li L, et al. Identification of fibroblast activation protein as an osteogenic suppressor and anti-osteoporosis drug target. Cell Rep. 2020;33(2):108252. https://doi.org/10.1016/j.celrep.2020.108252.
13. Zhang W, Dang K, Huai Y, Qian A. Osteoimmunology: the regulatory roles of T lymphocytes in osteoporosis. Front Endocrinol (Lausanne). 2020. https://doi.org/10.3389/fendo.2020.00465.
14. Sjögren K, Engdahl C, Henning P, Lerner UH, Tremaroli V, Lagerquist MK, et al. The gut microbiota regulates bone mass in mice. J Bone Miner Res. 2012;27(6):1357–67. https://doi.org/10.1002/jbmr.1588.
15. Novince CM, Whittow CR, Aartun JD, Hathaway JD, Poulides N, Chavez MB, et al. Commensal gut microbiota immunomodulatory actions in bone marrow and liver have catabolic effects on skeletal homeostasis in health. Sci Rep. 2017;7(1):5747. https://doi.org/10.1038/s41598-017-06126-x.
16. Uchida Y, Irie K, Fukuhara D, Kataoka K, Hattori T, Ono M, et al. Commensal microbiota enhance both osteoclast and osteoblast activities. Molecules. 2018;23(7):1517. https://doi.org/10.3390/molecules23071517.
17. Schwarzer M, Makki K, Storelli G, Machuca-Gayet I, Srutkova D, Hermanova P, et al. Lactobacillus plantarum strain maintains growth of infant mice during chronic undernutrition. Science. 2016;351(6275):854–7. https://doi.org/10.1126/science.aad8588.
18. Yan J, Herzog JW, Tsang K, Brennan CA, Bower MA, Garrett WS, et al. Gut microbiota induce IGF-1 and promote bone formation and growth. Proc Natl Acad Sci U S A. 2016;113(47):E7554–63. https://doi.org/10.1073/pnas.1607235113.
19. Cox LM, Yamanishi S, Sohn J, Alekseyenko AV, Leung JM, Cho I, et al. Altering the intestinal microbiota during a critical developmental window has lasting metabolic consequences. Cell. 2014;158(4):705–21. https://doi.org/10.1016/j.cell.2014.05.052.
20. Cho I, Yamanishi S, Cox L, Methé BA, Zavadil J, Li K, et al. Antibiotics in early life alter the murine colonic microbiome and adiposity. Nature. 2012;488(7413):621–6. https://doi.org/10.1038/nature11400.
21. Nobel YR, Cox LM, Kirigin FF, Bokulich NA, Yamanishi S, Teitler I, et al. Metabolic and metagenomic outcomes from early-life pulsed antibiotic treatment. Nat Commun. 2015;6:7486. https://doi.org/10.1038/ncomms8486.
22. Tyagi AM, Darby TM, Hsu E, Yu M, Pal S, Dar H, et al. The gut microbiota is a transmissible determinant of skeletal maturation. Elife. 2021;10:e64237. https://doi.org/10.7554/eLife.64237.

23. Liu JH, Chen CY, Liu ZZ, Luo ZW, Rao SS, Jin L, et al. Extracellular vesicles from child gut microbiota enter into bone to preserve bone mass and strength. Adv Sci (Weinh). 2021;8(9):2004831. https://doi.org/10.1002/advs.202004831.
24. Lucas S, Omata Y, Hofmann J, Böttcher M, Iljazovic A, Sarter K, et al. Short-chain fatty acids regulate systemic bone mass and protect from pathological bone loss. Nat Commun. 2018;9(1):55. https://doi.org/10.1038/s41467-017-02490-4.
25. Lee MJ, Chen Y, Huang YP, Hsu YC, Chiang LH, Chen TY, et al. Exogenous polyamines promote osteogenic differentiation by reciprocally regulating osteogenic and adipogenic gene expression. J Cell Biochem. 2013;114(12):2718–28. https://doi.org/10.1002/jcb.24620.
26. Liu Y, Yang R, Liu X, Zhou Y, Qu C, Kikuiri T, et al. Hydrogen sulfide maintains mesenchymal stem cell function and bone homeostasis via regulation of Ca(2+) channel sulfhydration. Cell Stem Cell. 2014;15(1):66–78. https://doi.org/10.1016/j.stem.2014.03.005.
27. Yu M, Malik Tyagi A, Li JY, Adams J, Denning TL, Weitzmann MN, et al. PTH induces bone loss via microbial-dependent expansion of intestinal TNF(+) T cells and Th17 cells. Nat Commun. 2020;11(1):468. https://doi.org/10.1038/s41467-019-14148-4.
28. Tyagi AM, Yu M, Darby TM, Vaccaro C, Li JY, Owens JA, et al. The microbial metabolite butyrate stimulates bone formation via T regulatory cell-mediated regulation of WNT10B expression. Immunity. 2018. https://doi.org/10.1016/j.immuni.2018.10.013.
29. Li JY, Chassaing B, Tyagi AM, Vaccaro C, Luo T, Adams J, et al. Sex steroid deficiency-associated bone loss is microbiota dependent and prevented by probiotics. J Clin Invest. 2016. https://doi.org/10.1172/jci86062.
30. Li JY, Yu M, Pal S, Tyagi AM, Dar H, Adams J, et al. Parathyroid hormone-dependent bone formation requires butyrate production by intestinal microbiota. J Clin Invest. 2020. https://doi.org/10.1172/jci133473.
31. Sabater González M. Skeletal bone structure and repair in small mammals, birds, and reptiles. Vet Clin North Am Exot Anim Pract. 2019. https://doi.org/10.1016/j.cvex.2019.01.002.
32. van de Velde JP, Vermeiden JP, Bloot AM. Medullary bone matrix formation, mineralization, and remodeling related to the daily egg-laying cycle of Japanese quail: a histological and radiological study. Bone. 1985. https://doi.org/10.1016/8756-3282(85)90322-9.
33. Rodriguez-Navarro AB, McCormack HM, Fleming RH, Alvarez-Lloret P, Romero-Pastor J, Dominguez-Gasca N, et al. Influence of physical activity on tibial bone material properties in laying hens. J Struct Biol. 2018. https://doi.org/10.1016/j.jsb.2017.10.011.
34. Fleming RH, McCormack HA, McTeir L, Whitehead CC. Medullary bone and humeral breaking strength in laying hens. Res Vet Sci. 1998. https://doi.org/10.1016/s0034-5288(98)90117-5.
35. Kerschnitzki M, Zander T, Zaslansky P, Fratzl P, Shahar R, Wagermaier W. Rapid alterations of avian medullary bone material during the daily egg-laying cycle. Bone. 2014. https://doi.org/10.1016/j.bone.2014.08.019.
36. Chen C, Turner B, Applegate TJ, Litta G, Kim WK. Role of long-term supplementation of 25-hydroxyvitamin D(3) on egg production and egg quality of laying hen. Poult Sci. 2020. https://doi.org/10.1016/j.psj.2020.09.020.
37. Bello A, Dersjant-Li Y, Korver DR. Effects of dietary calcium and available phosphorus levels and phytase supplementation on performance, bone mineral density, and serum biochemical bone markers in aged white egg-laying hens. Poult Sci. 2020. https://doi.org/10.1016/j.psj.2020.06.082.
38. Canoville A, Schweitzer MH, Zanno L. Identifying medullary bone in extinct avemetatarsalians: challenges, implications and perspectives. Philos Trans R Soc Lond B Biol Sci. 2020. https://doi.org/10.1098/rstb.2019.0133.
39. Pan D, Yu Z. Intestinal microbiome of poultry and its interaction with host and diet. Gut microbes. 2014. https://doi.org/10.4161/gmic.26945.
40. Liu Y, Feng Y, Yang X, Lv Z, Li P, Zhang M, et al. Mining chicken ileal microbiota for immunomodulatory microorganisms. ISME J. 2023. https://doi.org/10.1038/s41396-023-01387-z.
41. Lyu Z, Li H, Li X, Wang H, Jiao H, Wang X, et al. Fibroblast growth factor 23 inhibits osteogenic differentiation and mineralization of chicken bone marrow mesenchymal stem cells. Poult Sci. 2023. https://doi.org/10.1016/j.psj.2022.102287.
42. Wei F, Yang X, Zhang M, Xu C, Hu Y, Liu D. Akkermansia muciniphila enhances egg quality and the lipid profile of egg yolk by improving lipid metabolism. Front Microbiol. 2022. https://doi.org/10.3389/fmicb.2022.927245.
43. Xu C, Wei F, Yang X, Feng Y, Liu D, Hu Y. Lactobacillus salivarius CML352 isolated from Chinese local breed chicken modulates the gut microbiota and improves intestinal health and egg quality in late-phase laying Hens. Microorganisms. 2022. https://doi.org/10.3390/microorganisms10040726.
44. Demontiero O, Vidal C, Duque G. Aging and bone loss: new insights for the clinician. Ther Adv Musculoskelet Dis. 2012. https://doi.org/10.1177/1759720x11430858.
45. Bain MM, Nys Y, Dunn IC. Increasing persistency in lay and stabilising egg quality in longer laying cycles. What are the challenges? Br Poult Sci. 2016. https://doi.org/10.1080/00071668.2016.1161727.
46. Hadley JA, Horvat-Gordon M, Kim WK, Praul CA, Burns D, Leach RM Jr. Bone sialoprotein keratan sulfate proteoglycan (BSP-KSPG) and FGF-23 are important physiological components of medullary bone. Comp Biochem Physiol A Mol Integr Physiol. 2016. https://doi.org/10.1016/j.cbpa.2015.12.009.
47. Evans JM, Morris LS, Marchesi JR. The gut microbiome: the role of a virtual organ in the endocrinology of the host. J Endocrinol. 2013. https://doi.org/10.1530/joe-13-0131.
48. Husted AS, Trauelsen M, Rudenko O, Hjorth SA, Schwartz TW. GPCR-mediated signaling of metabolites. Cell Metab. 2017. https://doi.org/10.1016/j.cmet.2017.03.008.
49. Schwiertz A, Hold GL, Duncan SH, Gruhl B, Collins MD, Lawson PA, et al. Anaerostipes caccae gen. nov., sp. nov., a new saccharolytic, acetate-utilising, butyrate-producing bacterium from human faeces. Syst Appl Microbiol. 2002;25(1):46–51. https://doi.org/10.1078/0723-2020-00096.
50. Abdugheni R, Wang W-Z, Wang Y-J, Du M-X, Liu F-L, Zhou N, et al. Metabolite profiling of human-originated Lachnospiraceae at the strain level. iMeta. 2022;1(4):e58. https://doi.org/10.1002/imt2.58.
51. Yan J, Takakura A, Zandi-Nejad K, Charles JF. Mechanisms of gut microbiota-mediated bone remodeling. Gut microbes. 2018. https://doi.org/10.1080/19490976.2017.1371893.
52. Hernandez CJ, Beaupré GS, Carter DR. A theoretical analysis of the relative influences of peak BMD, age-related bone loss and menopause on the development of osteoporosis. Osteoporos Int. 2003. https://doi.org/10.1007/s00198-003-1454-8.
53. Whitehead CC. Overview of bone biology in the egg-laying hen. Poult Sci. 2004. https://doi.org/10.1093/ps/83.2.193.
54. Hiyama S, Yokoi M, Akagi Y, Kadoyama Y, Nakamori K, Tsuga K, et al. Osteoclastogenesis from bone marrow cells during estrogen-induced medullary bone formation in Japanese quails. J Mol Histol. 2019. https://doi.org/10.1007/s10735-019-09835-x.
55. Squire ME, Veglia MK, Drucker KA, Brazeal KR, Hahn TP, Watts HE. Estrogen levels influence medullary bone quantity and density in female house finches and pine siskins. Gen Comp Endocrinol. 2017. https://doi.org/10.1016/j.ygcen.2016.12.015.
56. Deng YF, Chen XX, Zhou ZL, Hou JF. Letrozole inhibits the osteogenesis of medullary bone in prelay pullets. Poult Sci. 2010. https://doi.org/10.3382/ps.2010-00632.
57. Takayanagi H. Osteoimmunology: shared mechanisms and crosstalk between the immune and bone systems. Nat Rev Immunol. 2007. https://doi.org/10.1038/nri2062.
58. Fujisaki J, Wu J, Carlson AL, Silberstein L, Putheti P, Larocca R, et al. In vivo imaging of Treg cells providing immune privilege to the haematopoietic stem-cell niche. Nature. 2011. https://doi.org/10.1038/nature10160.
59. Luo CY, Wang L, Sun C, Li DJ. Estrogen enhances the functions of CD4(+)CD25(+)Foxp3(+) regulatory T cells that suppress osteoclast differentiation and bone resorption in vitro. Cell Mol Immunol. 2011. https://doi.org/10.1038/cmi.2010.54.
60. Taylor A, Verhagen J, Blaser K, Akdis M, Akdis CA. Mechanisms of immune suppression by interleukin-10 and transforming growth factor-beta: the role of T regulatory cells. Immunology. 2006. https://doi.org/10.1111/j.1365-2567.2006.02321.x.
61. Grafe I, Alexander S, Peterson JR, Snider TN, Levi B, Lee B, et al. TGF-β family signaling in mesenchymal differentiation. Cold Spring Harb Perspect Biol. 2018. https://doi.org/10.1101/cshperspect.a022202.
62. Ciucci T, Ibáñez L, Boucoiran A, Birgy-Barelli E, Pène J, Abou-Ezzi G, et al. Bone marrow Th17 TNFα cells induce osteoclast differentiation, and link bone destruction to IBD. Gut. 2015. https://doi.org/10.1136/gutjnl-2014-306947.
63. Sato K, Suematsu A, Okamoto K, Yamaguchi A, Morishita Y, Kadono Y, et al. Th17 functions as an osteoclastogenic helper T cell subset that links T

cell activation and bone destruction. J Exp Med. 2006. https://doi.org/10.1084/jem.20061775.
64. Li Z, Li Q, Wang SJ, Zhang L, Qiu JY, Wu Y, et al. Rapid increase of carbonate in cortical bones of hens during laying period. Poult Sci. 2016. https://doi.org/10.3382/ps/pew182.
65. Prum RO, Berv JS, Dornburg A, Field DJ, Townsend JP, Lemmon EM, et al. A comprehensive phylogeny of birds (Aves) using targeted next-generation DNA sequencing. Nature. 2015. https://doi.org/10.1038/nature15697.
66. Wang S, Hu Y, Wu Y, Liu Y, Liu G, Yan Z, et al. Influences of bioapatite mineral and fibril structure on the mechanical properties of chicken bone during the laying period. Poult Sci. 2019. https://doi.org/10.3382/ps/pez474.
67. Huang R, Liu P, Bai Y, Huang J, Pan R, Li H, et al. Changes in the gut microbiota of osteoporosis patients based on 16S rRNA gene sequencing: a systematic review and meta-analysis. J Zhejiang Univ Sci B. 2022. https://doi.org/10.1631/jzus.B2200344.
68. Hill C, Guarner F, Reid G, Gibson GR, Merenstein DJ, Pot B, et al. Expert consensus document. The international scientific association for probiotics and prebiotics consensus statement on the scope and appropriate use of the term probiotic. Nat Rev Gastroenterol Hepatol. 2014. https://doi.org/10.1038/nrgastro.2014.66.
69. Koh A, De Vadder F, Kovatcheva-Datchary P, Bäckhed F. From dietary fiber to host physiology: short-chain fatty acids as key bacterial metabolites. Cell. 2016. https://doi.org/10.1016/j.cell.2016.05.041.
70. Chen S, Huang L, Liu B, Duan H, Li Z, Liu Y, et al. Dynamic changes in butyrate levels regulate satellite cell homeostasis by preventing spontaneous activation during aging. SCIENCE CHINA Life Sciences. 2023. https://doi.org/10.1007/s11427-023-2400-3.
71. He J, Chu Y, Li J, Meng Q, Liu Y, Jin J, et al. Intestinal butyrate-metabolizing species contribute to autoantibody production and bone erosion in rheumatoid arthritis. Sci Adv. 2022. https://doi.org/10.1126/sciadv.abm1511.
72. Chen TH, Chen WM, Hsu KH, Kuo CD, Hung SC. Sodium butyrate activates ERK to regulate differentiation of mesenchymal stem cells. Biochem Biophys Res Commun. 2007. https://doi.org/10.1016/j.bbrc.2007.02.057.
73. Katono T, Kawato T, Tanabe N, Suzuki N, Iida T, Morozumi A, et al. Sodium butyrate stimulates mineralized nodule formation and osteoprotegerin expression by human osteoblasts. Arch Oral Biol. 2008. https://doi.org/10.1016/j.archoralbio.2008.02.016.
74. Marsh AG, Sanchez TV, Midkelsen O, Keiser J, Mayor G. Cortical bone density of adult lacto-ovo-vegetarian and omnivorous women. J Am Diet Assoc. 1980;76(2):148–51.
75. Rivas A, Romero A, Mariscal-Arcas M, Monteagudo C, Feriche B, Lorenzo ML, et al. Mediterranean diet and bone mineral density in two age groups of women. Int J Food Sci Nutr. 2013. https://doi.org/10.3109/09637486.2012.718743.
76. Feehley T, Plunkett CH, Bao R, Choi Hong SM, Culleen E, Belda-Ferre P, et al. Healthy infants harbor intestinal bacteria that protect against food allergy. Nat Med. 2019. https://doi.org/10.1038/s41591-018-0324-z.
77. Montalban-Arques A, Katkeviciute E, Busenhart P, Bircher A, Wirbel J, Zeller G, et al. Commensal Clostridiales strains mediate effective anti-cancer immune response against solid tumors. Cell Host Microbe. 2021. https://doi.org/10.1016/j.chom.2021.08.001.

Publisher's Note